



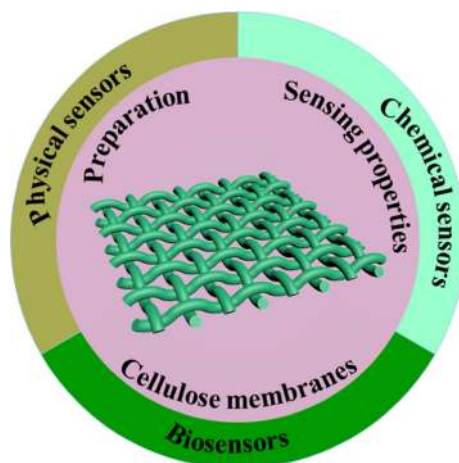
Recent advances in cellulose-based membranes for their sensing applications

Jiang Fan · Sufeng Zhang · Fei Li · Yonglin Yang · Min Du

Received: 14 May 2020 / Accepted: 7 September 2020 / Published online: 11 September 2020
© Springer Nature B.V. 2020

Abstract In recent years, sensing applications have played a very important role in various fields. As a novel natural material, cellulose-based membranes with many merits can be served as all kinds of sensors. This review summarizes the recent progress of cellulose membranes as sensors, mainly focusing on their preparation processes and sensing properties. In addition, the opportunities and challenges of cellulose membrane-based sensors are also prospected. This review provides some references for the design of cellulose membrane materials for sensing applications in the future.

Graphic abstract



J. Fan · S. Zhang (✉) · M. Du
Shaanxi Provincial Key Laboratory of Papermaking
Technology and Specialty Paper Development, National
Demonstration Center for Experimental Light Chemistry
Engineering Education, Key Laboratory of Paper Based
Functional Materials of China National Light Industry,
Shaanxi University of Science and Technology,
Xi'an 710021, People's Republic of China
e-mail: zhangsufeng@sust.edu.cn

F. Li
The Second Kindergarten, Economic and Technological
Development Zone, Xi'an 710021, People's Republic of
China

Y. Yang
School of Environmental Science and Engineering,
Shaanxi University of Science and Technology,
Xi'an 710021, People's Republic of China

Keywords Cellulose membranes · Sensing ·
Preparation · Properties

Introduction

Sensors are widely used in various areas of social development and human life, such as industrial production, agricultural planting, environmental detection and disease diagnosis (Ghoneim et al. 2019). According to the changes of environmental factors, sensors can be divided into three categories:

physical sensors that respond to pressure/strain, temperature and humidity; chemical sensors that respond to metal cations, non-metal ions, pH, gas/vapor and toxic organic compounds; and biosensors that respond to biomolecules and pathogens (Dai et al. 2020; Zhang et al. 2020; Fan et al. 2020a, b). At present, although the traditional instrument analysis methods have the merits of sensitivity and professionalism, they still exhibit some drawbacks: expensive instruments, complicated operation steps and professional operators. Therefore, the development of green, convenient, rapidly responding, multifunctional, highly sensitive and selective sensors is urgently needed.

Due to their various advantages of portable, real-time detection and flexible, the membrane materials have aroused a widespread interest of researchers. Until now, membrane materials are mainly inorganic matrices (e.g. metal oxides and ceramics) and organic substrates (Lee et al. 2019; Bassyouni et al. 2019; Weishaupt et al. 2020). However, inorganic matrices have the disadvantages of high cost, difficult processing and small market application scale, while organic substrates exhibit the advantages of low cost, easy processing and large market application scale. As a new organic and green substrate, cellulose-based membranes possess a series of advantages of environmentally friendly, excellent biodegradability and compatibility, which are extensively applied to sensing fields (Dai et al. 2020). Cellulose membranes are mainly prepared by vacuum filtration, solution regeneration, electrospinning, solution casting, phase inversion and other preparation methods (Mautner 2020; Douglass et al. 2017; Thakur and Voicu 2016). The raw materials for cellulose membranes preparation can include ethyl cellulose, cellulose nanofibers, cellulose nanocrystals, cellulose acetate, triacetyl cellulose, sodium carboxymethyl cellulose, nitrocellulose, etc. (Fu et al. 2019; Zhu et al. 2019a, b; Li et al. 2017a, b, c; Amin 2015; Duong et al. 2018; Hittini et al. 2020; Tang et al. 2019). The excellent sensing performances can be obtained by introducing metal nanowires, metal nanoparticles, carbon dots, quantum dots, carbon nanotubes, fluorophores, organic dyes and antigen-antibodies into cellulose membranes through physical-chemical methods (Lou et al. 2020; Zhang et al. 2019a, b, c; Jiang et al. 2020a, b; Li et al. 2017a, b, c; Lv et al. 2019a, b; Shankar et al. 2020).

As far as we know, there are a few reviews on cellulose-based membranes for sensing applications.

In this review, we summarize the recent developments of cellulose-based membranes as physical sensors, chemical sensors and biosensors over the past five years. As well, the challenges and development prospects of cellulose membrane-based sensors are briefly discussed.

Physical sensors

Pressure/strain sensors

With the acceleration of life rhythm and pressure, real-time human motion sensing and pulse monitoring become increasingly important. Body motions can fully reflect the physiological states of human body. Pulse wave is closely related to various physiological diseases, which is of great significance to evaluate the health status of the body and prevent diseases. At present, traditional approaches of visual method, sound method and oscillometric method are mainly used for body motion sensing and pulse monitoring, which exist many deficiencies of complex structure, complicated fabrication process, required external power, trained technicians, poor portability and compatibility, etc. (Yang et al. 2019; Regev and Wulich 2019). Therefore, it is urgent to develop simple, dynamic, timely, sensitive, breathable, wearable and energy-sustainable pressure sensors for monitoring body motion and pulse wave.

Li Zhaoling and co-workers developed a self-powered and triboelectric all-fiber structured pressure sensor via the electrospinning technique, which was consisted of polyvinylidene fluoride/silver nanowires nanofibrous membrane (PVDF/Ag NWs NFM) as the negatively triboelectric layer, ethyl cellulose nanofibrous membrane (EC NFM) as the positively triboelectric layer and two layers of conductive fabrics on the flexible polydimethylsiloxane (PDMS) substrate (Fig. 1a) (Lou et al. 2020). The incorporation of hierarchically rough structure into the nanofibers could improve the sensing performances of this wearable sensor, which could be prepared by phase separation approach using mixed solutions with different solvent ratios. Furthermore, the triboelectric properties of the nanofibrous membranes had an important influence on the sensitivity of pressure sensor. The results demonstrated that the sensing mechanism of this pressure sensor in the approaching/

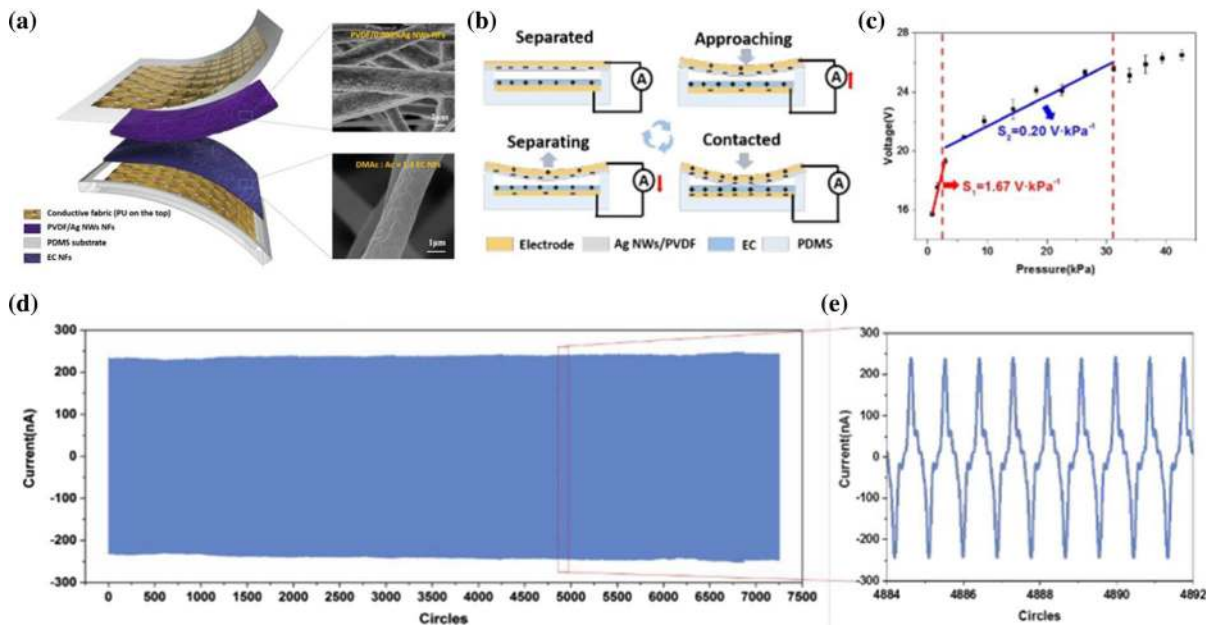


Fig. 1 **a** The structural design of this pressure sensor textile. **b** Working mechanisms of the pressure sensor. **c** Electrical signals in term of output voltage as a function of the applied

separating mode was attributed to the effects of contact electrification and electrostatic induction (Fig. 1b). A pressure range (0–3 kPa) with LOD (limit of detection) of 1.67 V kPa^{-1} and a pressure range (3–32 kPa) with LOD of 0.20 V kPa^{-1} were obtained (Fig. 1c). After 7200 cycles' of continuous operation, the current output of this sensor did not even show obvious changes, which showed that the pressure device had an excellent stability (Fig. 1d). In addition, the pressure sensor can work in a self-powered manner for detecting and quantifying various human motions on different body parts, such as elbows, knees and ankles. This high-performance pressure-sensitive membrane can be extensively applied for wearable electronics and artificial intelligence areas.

Carbon nanotubes (CNTs) with a cylindrical nanostructure have excellent physical properties, which can be widely used in the field of conductive films (Jheng et al. 2019). Lokendra Pal and co-workers developed a capacitive pressure sensor, by placing a piece of insulating crepe paper between two layers of cellulose nanofibers/multi-walled carbon nanotubes (CNF/MWCNTs) membranes (Zhang et al. 2019a, b, c). When MWCNTs content was 5 wt%, this CNF/MWCNTs membranes showed excellent electrical conductivity (Fig. 2e). However, when an

pressure. **d** Sensing stability test of the pressure sensor under around 7200 working cycles. Adapted with permission from Lou et al. (2020), Copyright 2020, American Chemical Society

external pressure acted on the pressure sensor, the capacitance of the sensors increased with the decrease of the distance between the conductive CNF/MWCNTs membranes (Fig. 2d). When the pressure was removed, the shape of the sensor returned to its original status due to the inherent stiffness and elasticity of the crepe paper. Moreover, the capacitive pressure sensor exhibited an almost linear relationship on the pressure range from 0 to 10 kPa. This conductive membrane provided a great practical potential in electronics applications (e.g. touch screens).

Sun Yueming and co-workers prepared a well-aligned reduced graphene oxide/electrospun cellulose acetate nanofibers (RGO/CA) film as a strain sensor through a facile hot-pressing procedure (Fu et al. 2019). An ordered fibrous membrane can be obtained by a rotation drum collector. By using the hot-pressing technique, not only GO can be reduced to RGO, but also the mechanical properties and conductivities of the RGO/CA film can be enhanced. More importantly, these RGO/CA conductive membranes can be used as strain sensors in a broad deformation range and with versatile deformation types, such as bending and pushing. A strain sensor based on carbon nanotubes/cellulose nanocrystals/electrospun polyurethane membranes was designed by Fu Qiang and

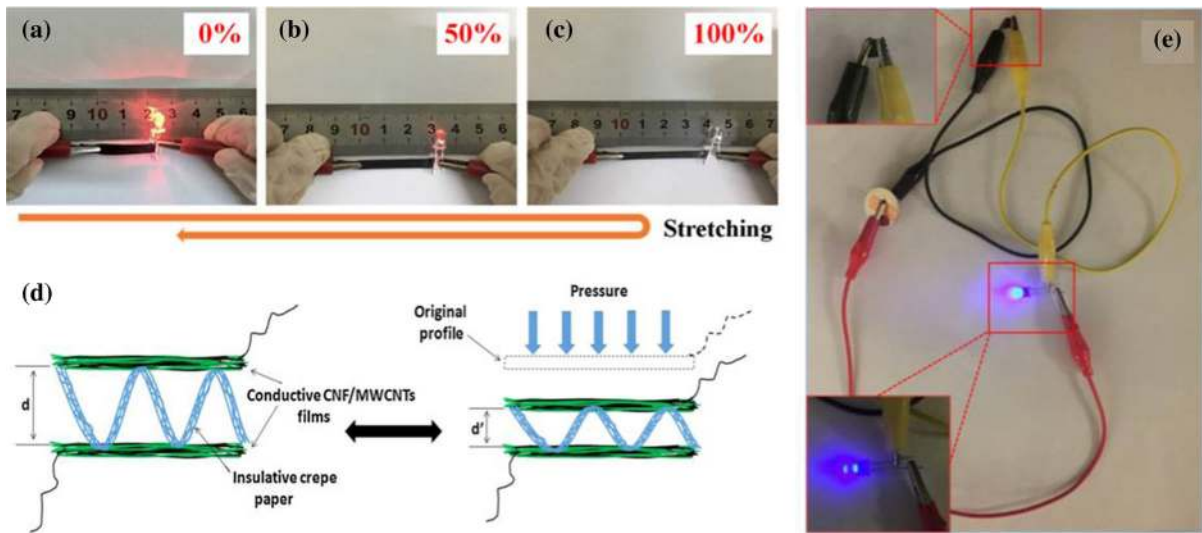


Fig. 2 a–c Visual controlling and the different brightness of a LED indicator under different applied strains by using the strain sensor. Adapted with permission from Zhu et al. (2019a), Copyright 2019, American Chemical Society. **d** Schematic mechanism of the capacitor after being placed under pressure.

e Photographic image of the circuit consisted of the CNF/MWCNTs membranes with 5 wt% MWCNTs. Adapted with permission from Zhang et al. (2019a), Copyright 2019, Elsevier B.V.

co-workers through one-step simple filtration method (Zhu et al. 2019a, b). When the loadings were below 20 mL, the sensitivities of these sensors improved with the increase of CNT-CNC loadings. When the filler volume was 10 mL, this strain sensor showed a tolerable strain of 500% without broken and high sensitivity (gauge factor = 321). The brightness of the LED was regulated by this strain sensor, which turned darker with the increase of strain (Fig. 2ac). More interesting, this strain sensor can be applied for monitoring of full-range of human body motions, including phonation, respiration and finger bending, etc. This strain sensor provided an ideal strategy of versatile applications (e.g. human motion detection, electronic skin, intelligent electronics).

Temperature sensors

Temperature is an important thermodynamic parameter, which affects almost all physicochemical phenomena and chemical reactions (Mazza and Raymo 2019). Therefore, it is very important to monitor the temperature of human activities, the growth of animals and plants, various industrial processes and broad fields (e.g. aerodynamics, meteorology, oceanography and military). Traditional temperature sensing methods have been reported, such as volume expansion

thermometers, infrared thermometers and other thermocouples, which existed their own intrinsic defects of only measurement of the object surfaces, poor spatial resolution and interference of strong electric and magnetic fields. Thus, it is necessary to design temperature sensors with high sensitivity, long-term stability, fast response, low cost and wide working range.

Rare-earth materials and carbon dots (CDs) have temperature-induced dependencies, which can be applied to temperature sensing (Zhang et al. 2019a, b, c; Jiang et al. 2020a, b). The flexible isotropic films for temperature sensing were prepared by Chen Zhilin and co-workers, which were based on cellulose nanocrystal (CNC)-assisted CDs-grafted SAO (SrAl_2O_4 , Eu^{2+} , Dy^{3+}), and subsequently modified with amino-silane and nanofibrillated cellulose skeletons (Fig. 3a) (Zhang et al. 2019a, b, c). The increase of temperature promoted non-radiant channels of surface defect (or trap) states, thus reduced the PL emission intensity. There was an excellent linear correlation between temperature (243–383 K) and $\text{PL}(506)/(452)$, with the sensitivities of ONFC/ NH_2 @CNC-CDs@SAO sensing film ($0.257\% \text{ K}^{-1}$) and CDs-dipping ONFC sensing film ($0.270\% \text{ K}^{-1}$) at 383K, respectively. Besides, this film exhibited high light-induced scattering, good flexibility and

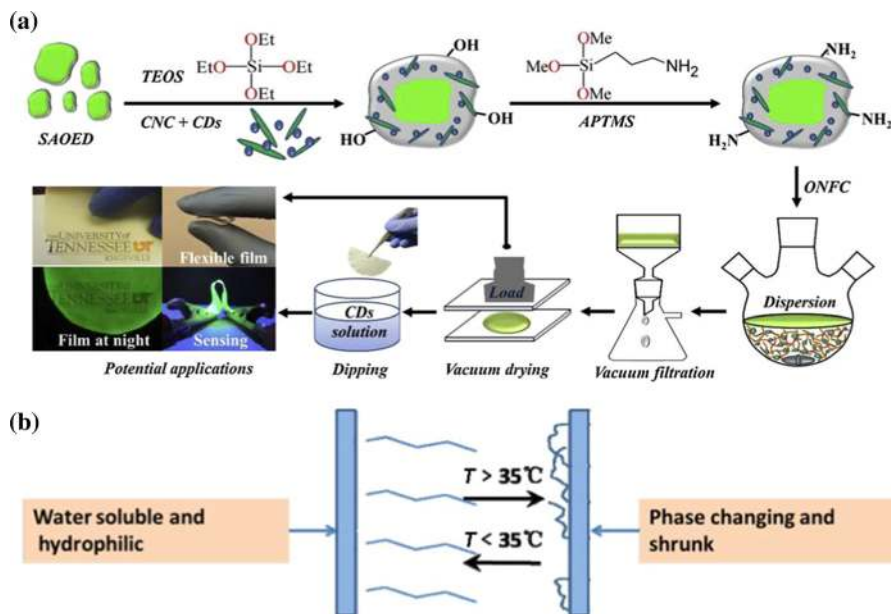


Fig. 3 **a** Schematic illustration of the preparation of flexible ONFC fluorescent scattering films for temperature sensing. Adapted with permission from Zhang et al. (2019c), Copyright 2019, Elsevier B.V. **b** The mechanism of temperature

responsiveness of the membrane. Adapted with permission from Li et al. (2017c), Copyright 2019, Wiley-VCH Verlag GmbH & Co. KGaA

reversibility. Jaehwan Kim and co-workers developed a reduced graphene oxide (rGO)/cellulose composite film as a temperature sensor (Sadasivuni et al. 2015). According to tunneling conduction mechanisms, the capacitance of these films increased with the increase of temperature. These films can be served as excellent candidates for temperature monitoring in the future practical applications.

A novel cellulose acetate (CA) ultrafiltration membrane modified with block copolymer polyethylene oxide-polypropylene oxide-polyethylene oxide/poly(2-(dimethylamino) ethyl methacrylate) F127-b-PDMAEMA through phase inversion method was prepared by Zhou Jiancheng and co-workers, with stimuli-responsiveness to temperature (Li et al. 2017a, b, c). As an amphiphilic additive, F127-b-PDMAEMA can change the pore structure of this membrane and improve their porosity, which can contribute to increase the sensitivity of this membrane towards temperature. When the temperature was higher than 35 °C, the pure water fluxes of this membrane increased obviously. When the temperature was higher than the lower critical solution temperature LCST (35 °C), PDMAEMA shrunk and released the place for the membrane pores. However, when it was

lower than LCST, PDMAEMA extended, subsequently occupied the space and made the pores smaller (Fig. 3b). Besides, this membrane also had a stimuli-responsive effect on pH (2–14). However, the performances of this temperature-sensing membrane were still unsatisfied, and more novel high quality temperature-responsive cellulose-based membranes should be urgently developed.

Humidity sensors

Relative humidity measurement is very important in the fields of meteorology, industrial process control, agricultural planting and food storage. Moreover, the measurement of human body humidity is of great significance to the evaluation of human health. According to the change of physical parameters after interaction with water molecules, humidity sensors can be divided into capacitance type, resistance type, impedance type, optical fiber type, etc. (Blank et al. 2016; Lv et al. 2019a, b). However, most of the commercially available humidity sensors were based on porous ceramics or metal oxides, which existed some shortcomings, such as the rigid structure, the complicated integration process, the restricted

accuracy and sensitivity under high temperature or humidity (Wang et al. 2016a, b; Shaheen et al. 2020). Therefore, it is vital to develop the humidity sensors with flexibility, wide response range, fast response, high sensitivity and low hysteresis.

A flexible cellulose nanofiber/carbon nanotube (NFC/CNT) humidity sensor was designed by Chen Gang and co-workers through vacuum filtration technique (Zhu et al. 2019a, b). The introduction of NFC can improve the humidity sensitive performance of CNTs network, because massive hydroxyl groups in cellulose molecular chains can firmly absorb water molecules. When CNT weight ratio was 5%, the current decreased almost linearly with the increase of relative humidity 11–95%. The NFC/CNT-5 wt % exhibited a high sensitivity with 69.9% at 95% relative humidity. In addition, this humidity film-sensor realized human breath monitoring at different rates (Fig. 4). A self-standing humidity sensor was prepared by Gary Chinga-Carrasco and co-workers through directly printed carbon-based interdigitated electrodes (IDEs) onto CNF/poly(ethylene glycol) (PEG) films (Syrový et al. 2019). PEG not only improved the mechanical properties of CNF films, but also had a

positive effect on the printing properties of CNF substrates. This film sensor demonstrated that the impedance decreased with the increase of relative humidity (20–90%). However, the longer response and recovery time of CNF/PEG film sensors were needed. These film sensors offered a potential humidity measurement method in scientific and industrial fields.

Chemical sensors

Metal cations sensors

Metal-ions pollution mainly comes from industrial, traffic and domestic waste, which has seriously threatened the safety of drinking water, industrial and agricultural water sources. Excessive intake of metal ions can lead to serious diseases and even death. However, the traditional instrument techniques for metal-ions measurement have various disadvantages, such as expensive instrument, complicated sample preparation procedure, time-consuming, long analysis time and professional operation. Therefore, the

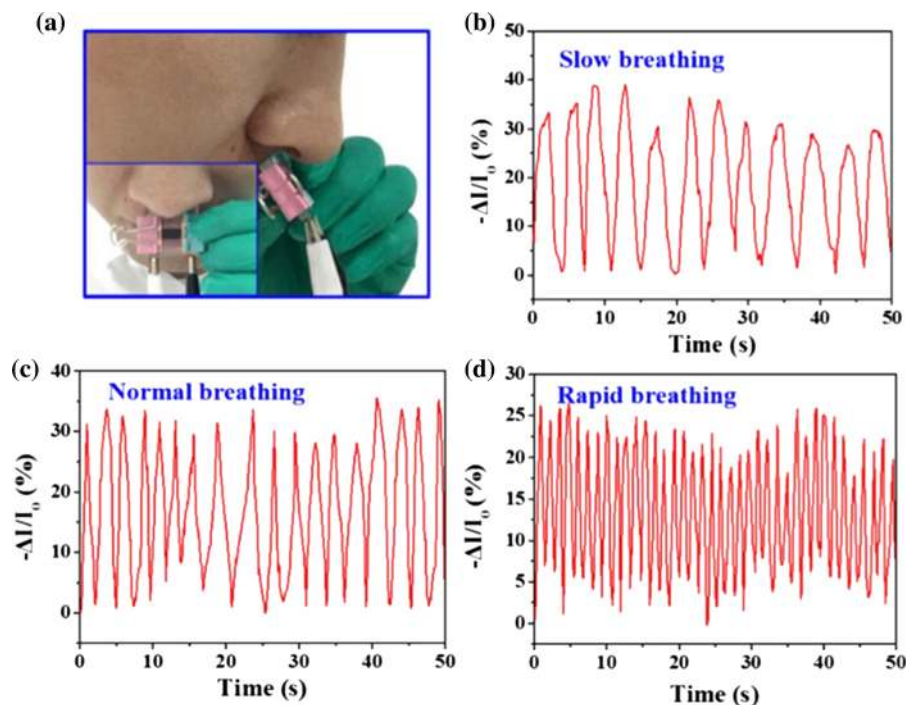


Fig. 4 The application of the NFC/CNT humidity sensor for human breath monitoring at **a**, **b** slow, **c** normal, **d** rapid frequency. Adapted with permission from Zhu et al. (2019b), Copyright 2019, American Chemical Society

development of green, fast, efficient, convenient, highly sensitive and selective methods for metal ions detection is particularly important.

Rhodamine derivatives can be served as various metal ions probes, because of their excellent photo-physical characteristics (Ye et al. 2020). A cellulose triacetate membrane immobilized Rhodamine 6G phenylthiosemicarbazide derivative (Rh6G-P) through room temperature solution casting method was prepared by Sangita D. Kumar and co-workers (Thakur et al. 2015). When the opening of spirolactum ring was induced by Hg^{2+} ions, the naked-eye color of the colorless membrane sensor turned pink (Fig. 5a). This sensor had successfully realized the

determination of Hg^{2+} ions in a wide linear range of 10–5000 ng/mL with LOD of 1.3 ng/mL. Similarly, 5-(2',4'-dimethylphenylazo)-6-hydroxy-pyrimidine-2,4-dione (DMPAHPD) can be acted as metal-ions probes (Amin and Ahmed 2010). Amin (2015) designed a triacetylcellulose membrane loaded with DMPAHPD dyes for detecting Hg^{2+} ions. The complex formation occurred between Hg^{2+} ions and this membrane, which led to the color change from orange to deep red. The membrane sensor exhibited a lower LOD of 0.3 ng/mL over a linear concentration range of 1.0–80 ng/mL. These proposed sensing membranes may be promising candidates for the determination of Hg^{2+} ions in the actual water samples.

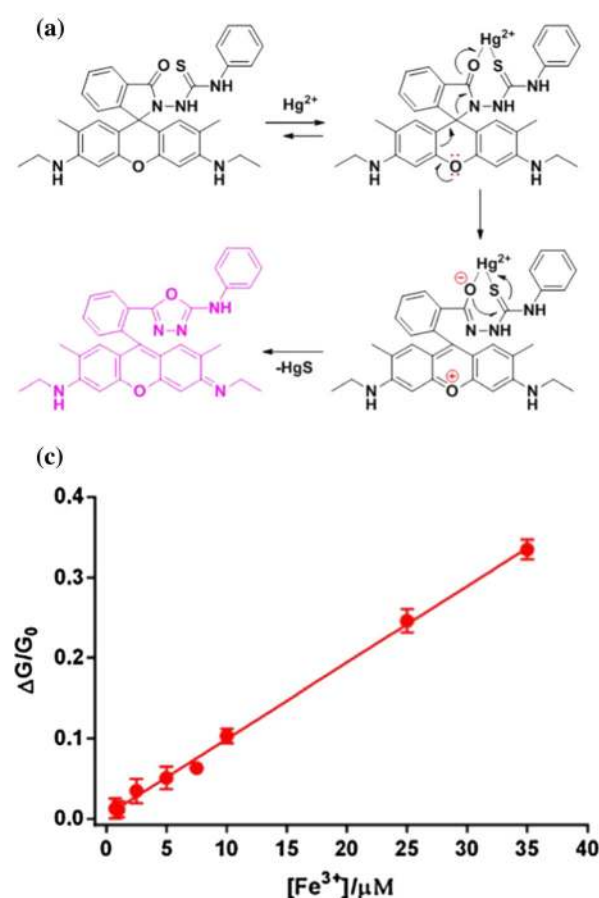
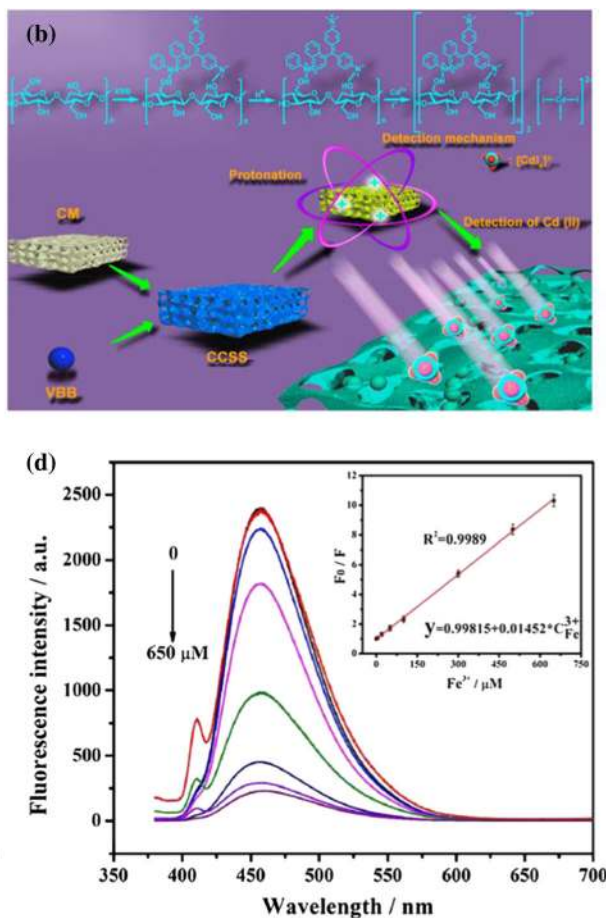


Fig. 5 a Hg^{2+} recognition mechanism by the incorporated Rh6G-P derivative in the optode. Adapted with permission from Thakur et al. (2015), Copyright 2015, Elsevier B.V. b Cd^{2+} ions detection mechanism with the sensor strips. Adapted with permission from Jiang et al. (2020a), Copyright 2020, American Chemical Society. c The relationship between colorimetric



response and Fe^{3+} concentrations. Adapted with permission from Li et al. (2017b), Copyright 2017, Elsevier B.V. d The FL intensity of the BC/N-GOQDs with different Fe^{3+} concentrations. Inset: The linear relationship between FL intensities and Fe^{3+} concentrations. Adapted with permission from Lv et al. (2019b), Copyright 2019, Springer

A cellulose membrane-based colorimetric sensor strip (CCSS) functionalized with victoria blue B (VBB, as an indicator) through intermolecular hydrogen bonds was developed by Luo Xiaogang and co-workers (Jiang et al. 2020a, b). Figure 5b showed design scheme of CCSS and detection mechanism of CCSS with Cd^{2+} ions. When added with Cd^{2+} , the color of CCSS was observed from yellow to blue-green by the naked eye. Moreover, a visual sensitivity limit 0.01 mg/L was obtained. This sensing system CCSS was successfully applied to discriminate Cd^{2+} in real waters.

Naphthalimide derivatives presented high fluorescence quantum yield, good photo-stability and long emission wavelength, which can be acted as metal ions sensors (Liu et al. 2020). Xiao Huining and co-workers constructed a green cellulose membrane (NGC), which coated with graphene oxide (GO) and naphthalimide molecule through hydrogen bonding and π - π stacking (Li et al. 2018). Because the coordination of piperazine units and Cu^{2+} ions blocked photo-induced electron transfer (PET) effect, the NGC membrane with Cu^{2+} appeared a strong fluorescence emission peak at 510 nm compared to the previously NGC membrane without Cu^{2+} . Besides, a detection limit 0.73 μM was achieved. CdTe quantum dots (CdTe QDs) can be worked as the sensing platform for metal ions detection (Elmizadeh et al. 2017). Wu Yiwei and co-workers synthesized a ratiometric fluorescent cellulose acetate membrane, which was immersed in CdTe QDs/graphite carbon nitride (GCNNs) solutions (He et al. 2020). With the increase of Cu^{2+} concentrations, the color of this membrane sensor was gradually changed from pink yellow to blue under UV lamp. Moreover, a wide semi-quantitative range (0.01–5.0 $\mu\text{g/mL}$) for Cu^{2+} detection was obtained. All these results suggested that the cellulose membranes offered a convenient, reliable method for on-site detection of Cu^{2+} ions in practical waters, such as red wine and drinking water.

Gold nanoparticles (AuNPs) have been widely used in sensing fields due to their excellent photo-physical properties (Rao et al. 2019). Hou Changjun designed a colorimetric paper-based membrane sensor through the process of TiO_2 modification, hydrophobic/hydrophilic coating, $-\text{NH}_2$ and $-\text{SH}$ groups decoration, and AuNPs immobilization (Li et al. 2017a, b, c). With the increase of Fe^{3+} concentrations, the original reddish intensity of the membrane gradually

decreased. In addition, a detection limit 0.85 μM was obtained with a linear relationship between colorimetric response and Fe^{3+} concentrations (1.0–37 μM) (Fig. 5c). Graphene oxide quantum dots (GOQDs) exhibited outstanding optoelectronic characteristics, which have attracted many interests in sensing areas (Park and Seo 2019). A bacterial cellulose/nitrogen-doped graphene oxide quantum dot-based fluorescent membrane (BC/N-GOQDs) through a one-step self-assembly and in situ cultivation strategy (via hydrogen bonding) was synthesized by Wei Qufu and co-workers (Lv et al. 2019a, b). The strong coordination of surface functional groups in BC/N-GOQDs and Fe^{3+} ions caused blue fluorescence quenching. More importantly, the BC/N-GOQDs sensor presented an outstanding selectivity for Fe^{3+} ions (0.5–650 μM) with an ultralow detection limit 69 nM (Fig. 5d). These cellulose membranes provided a potential for Fe^{3+} determination in real water samples (e.g. lake waters, serum and mineral waters).

A cellulose membrane functionalized with 1,4-dihydroxyanthraquinone (1,4-DHAQ) and carbon nanotubes (CNTs) was fabricated by Wang Meiling and co-workers (Gu et al. 2017). In the presence of Cu^{2+} ions, the fluorescence intensity of the 1, 4-DHAQ-doped CNTs@CL membrane decreased significantly. A linear range for Cu^{2+} detection (0–0.022 μM) and a detection limit 0.00217 μM was achieved. What is more surprising is that fluorescence emission was released when Cr^{3+} ions were added to the mixture of Cu^{2+} ions and 1,4-DHAQ-doped CNTs@CL membrane. Meanwhile, a linear equation of Cr^{3+} ions concentrations (0–0.024 μM) and LOD (0.00221 μM) was obtained. However, the presence of Cr^{3+} ions may interfere with the detection of Cr^{6+} ions. Rafal Sitko and co-workers prepared the amino-silanized cellulose membrane for realizing selective Cr^{6+} ions detection in the presence of Cr^{3+} (Jamroz et al. 2019). An excellent sensitivity with LOD of 0.16 ng/mL indicated that the membrane sensing system had a great promising in recognizing Cr^{6+} ions in real applications.

A colorimetric paper-based membrane sensor for Ni^{2+} determination was developed by Hou Changjun and co-workers, through a preparation procedure of TiO_2 coating, calcination, hexadecyltrimethoxysilane (HTDES) and hydrophilic modification (Li et al. 2017a, b, c). The membrane sensor using zincon/hollow ZnSiO_3 nanospheres/ Na_2 -EDTA solutions

presented a dynamic range (0.65–89 μM) and a calculated detection limit 0.68 μM . The color change of membrane sensor from pink to grey was attributed to indicator displacement mechanism. Silver staining technology is extensively applied to ultra-trace sensing fields because of its excellent signal amplification (Tang et al. 2010; Qi et al. 2010). A cellulose acetate membrane (CAM) decorating with dithizone (Dz) for detecting Pb^{2+} and Cd^{2+} ions was prepared by Zhao Yuandi and co-workers, with chemical bath deposition and silver stain technology (Wang et al. 2016a, b). The original gray color of the membrane sensor was changed to black (observing by naked-eye) when contacting with Pb^{2+} or Cd^{2+} ions. There was a linear fitting over $\text{Pb}^{2+}/\text{Cd}^{2+}$ concentrations (1–100 nM), and simultaneously an extremely low visual detection limit 1 nM was obtained. This chemosensor provided a convenient technique for $\text{Pb}^{2+}/\text{Cd}^{2+}$ detection in practical wastewaters.

Non-metal ions sensors

Chloride ions (Cl^-) permeation can cause the erosion of concrete buildings in harsh environments and then lead to reduction of the strength, utility and aesthetic quality of the concrete structure (Angst et al. 2009). Therefore, it is of great significance to monitor Cl^- ions in concrete environment. A novel fiber optic probe based on cellulose acetate (CA) film immobilizing lucigenin-doped silica nanoparticles via physical embedding was developed by Ding Liyun and co-workers (Xiao et al. 2019). This sensitive film can be served as a highly selective probe for detecting Cl^- ions in KCl solutions. Based on fluorescence quenching principle, a linear relationship between fluorescence intensity and Cl^- ions concentrations (0.02–0.06 M) was obtained (Fig. 6a). This material had various advantages of simplicity, convenience and efficiency in selective identification of Cl^- ions in building fields.

Nitrate ions (NO_3^-) can lead to the pollution of water systems (e.g. lakes, rivers, seas and oceans), because of the eutrophication of algae. Furthermore, nitrate is very harmful to human, especially to infant. Therefore, it is very urgent to realize the rapid detection of nitrate in water environment. Jong Il Rhee and co-workers reported an oxazine170 perchlorate-ethyl cellulose (O17-EC) membrane with a clay hydrotalcite (HT, working as a reducing reagent

for reduction of nitrate to ammonia) for colorimetric and ratiometric detection of nitrate (Duong et al. 2018). When the concentrations of nitrate increased from 0.1 mM to 10 mM, the color transition of the O17-HT-EC membrane was clearly observed under an excitation wavelength (470 nm) irradiation (Fig. 6b). The membrane sensor demonstrated a highly selective in the detection range (0.1–1.0 mM) with a sensitive detection limit 0.089 mM. Meanwhile, this sensor exhibited a fast response time (~ 10 s) and long-term stability (> 1 month) and outstanding reversibility, which suggested that the novel approach can recognize nitrate in real water samples instead of traditional methods (e.g. flow injection analysis and molecular emission cavity analysis).

Due to its toxicity and bioaccumulation, a high intake of Selenium(IV) can cause dangerous diseases to living organisms (Ventura et al. 2009). Thus, the development of a convenient and highly efficient method for determining Se(IV) is extremely important. Preeti Sunil Kulkarni prepared a cellulose triacetate plasticized membrane modified with tri-octyl methyl ammonium chloride (A1-336, as an ion exchanger) (Kulkarni et al. 2018). This sensor exhibited a highly selective for Se(IV), and was not influenced by the other interfering anions, such as oxalate, phosphate, nitrate, bicarbonate, bromate, and chloride. The sensing process can be briefly described as follows: first, iodometric method happened between Se(IV) and iodide ions in acidic medium (from colorless to yellow color); second, tri-iodide anion (I_3^-) reacted with variamine blue dye in sodium acetate solutions (from yellow to violet) (Fig. 6c). A good linear range (0.2–3 $\mu\text{g}/\text{mL}$) and LOD value (0.15 $\mu\text{g}/\text{mL}$) indicated that the material can be served as an ideal method for the determination of Se(IV) in pharmaceutical industries.

Excessive As(III) is related to a series diseases of cancers, diabetes and reproductive problems (Hao et al. 2009). A cellulose/amorphous silica/(3-mercaptopropyl)-trimethoxysilane membrane for highly selective adsorption and detection of As(III) was developed by Rafal Sitko and co-workers (Fig. 6d) (Lukojko et al. 2018). Due to the strong binding ability between As(III) and mercapto groups, this membrane material displayed excellent selectivity for ultra-trace As(III) detection in the presence of interfering ions, including As(V), heavy metals (e.g. Pb^{2+} , Ni^{2+} and Co^{2+}) and anions (e.g. SO_4^{2-} , NO_3^- and Cl^-). More

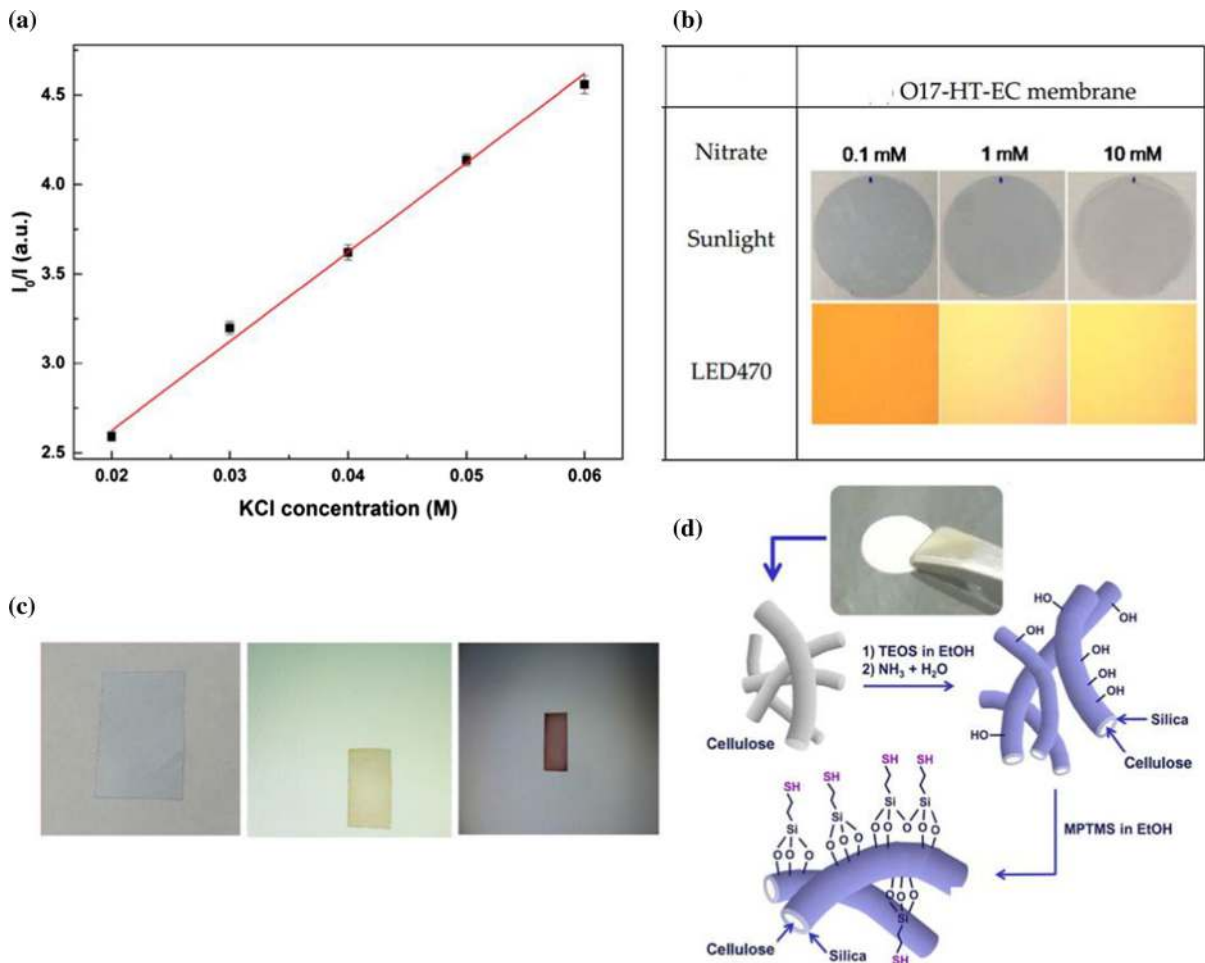


Fig. 6 **a** Calibration curve of optical fiber sensing probe response to Cl^- by KCl standard solutions. Adapted with permission from Xiao et al. (2019), Copyright 2019, Elsevier B.V. **b** The photo images of the O17-HT-EC membranes with different nitrate concentrations under sunlight or LED (470 nm) irradiation. Adapted with permission from Duong et al. (2018),

importantly, the miniaturized membrane achieved a linear range 0.2–200 ng/mL and an extremely low detection limit 0.045 ng/mL, which was considerably lower than the maximum allowable value 10 ng/mL of As(III) in drinking water according to World Health Organization. This novel sensing platform offered a solvent-free, low cost and environmental-friendly method in determination of As(III) in high salinity water. However, realizing efficient detection of As(V) is still a huge challenge.

The efficient combination of sensors with Internet of things (IOT) provides great potential for a stable renewable energy system (Bethke et al. 2018). Woo Soo

Copyright 2018, MDPI, Basel, Switzerland. **c** The color change of films sorbed with I_3^- and after treatment with variamine blue. Adapted with permission from Kulkarni et al. (2018), Copyright 2018, Springer. **d** The preparation process of cellulose/SiO₂/MPTMS membranes. Adapted with permission from Lukojko et al. (2018), Copyright 2018, Elsevier B.V.

Kim and co-workers constructed a 3D printed disposable wireless ion selective sensor for NH_4^+ detection, which was consisted of AgNWs, cellulose nanofibers and polyimide (Kim et al. 2019). Through measuring the magnitude of reflection coefficient S_{11} , the change of NH_4^+ concentrations on IS-LC sensor was wirelessly detected by VNA, and a high sensitivity of 3.4%/M was achieved. This 3D printed wearable ion sensor can provide an efficient method for the realization of Internet of things and wireless monitoring.

pH sensors

pH (hydrogen ion concentration) is closely related to most areas. pH value is not only a very important parameter in the industrial, pharmaceutical and food industries, but also has an influence on global ecology and physiological biochemistry (Chu et al. 2013; Koch et al. 2013; Gotor et al. 2017). Besides, pH plays an important role in many chemical and biological processes of animals, plants and bacteria. So far, three methods of electrochemical, photochemical sensors and pH test paper strips are mainly used to determine pH. Although pH test paper has the advantages of cheap, wide coverage and simple operation, it does not have high resolution. Even though pH glass electrode is the most commonly used pH sensor, it is still interfered by high temperature, high pressure, strong alkali, ionic strength, some organic matters and electromagnetic radiation. However, when the pH value changed, the optical sensor may read the changes of absorption, fluorescence or reflectivity. Besides, the optical pH sensor also had the advantages of anti-electromagnetic interference, convenient, low cost, high selectivity and sensitivity. In general, an optical pH sensor is mainly made of a pH indicator (acid-based indicators) and an organic carrier (e.g. hydrogel or cellulose) through adsorption, chemical bonding and sol–gel method.

Zhang Jianxin fabricated an optical pH sensitive membrane via sol–gel method, which was developed by embedding four indicators of congo red, bromophenol blue, cresol red and chlorophenol red into an organic carrier, simultaneously cross-linked by tetraethyl orthosilicate (TEOS) and cellulose acetate (Zhang and Zhou 2018). According to a linear relationship between Power (μW) and pH values, a working detection range (2.5–11.0) was obtained, with a measurement accuracy (0.2 pH) of the sensor. The sensing membrane had a wide response range to pH values, which was probably attributed to the interaction of the four indicators. Compared with traditional electric chemical electrodes, various advantages (e.g. good stability and repeatability) of this pH sensor provided a practical evaluation method in the areas of clinical medicine, biopharmaceutical and industrial sewage. However, the sensor needed a long response time and should be activated before normal measurement. Besides, the sensor cannot work well in strong acid ($\text{pH} \leq 2.5$) and alkali ($\text{pH} \geq 11.0$) environments.

A pH-responsive sensing platform was produced by Narges Chamkouri, by immobilizing phenol red on the triacetylcellulose membrane (Chamkouri 2015). With the increase of pH values, the absorbance at 464 nm of the optical sensor and detected solutions decreased. Their results showed that the pH sensor maintained a relatively wide linear range (3.0–12.0) with a long-term stability (8 months) in water/ethanol (50:50, v/v). In addition, a correlation coefficient (0.999) and relative standard deviations (less than 0.7%) supplied a good reliable and accurate platform for monitoring pH in the future applications.

Because the optical probes depended on indicator transition characteristics, they cannot be used for certain applications. Due to the advantages of high sensitivity and without frequent recalibration, the luminescent pH sensors had an extensively applicability to practical samples. Lanthanide (Ln) compounds with excellent photo-physical properties played a key role in these fields of luminescent labels, probes, phosphors and biological (Ning et al. 2019; Khullar et al. 2019). A luminescent pH membrane sensor based on cellulose acetate (CA) and a new europium complex (Eu^{3+} /theonyl trifluoroacetone/gallic acid/pyridine dicarboxylic acid) was prepared by Axel Duerkop and co-workers (Waleed Al-Qaysi and Duerkop 2018). With the increase of pH values (2–7), the fluorescence intensity at 615 nm of the sensing film increased significantly, which was related to the $\text{p}K_{\text{a}}$ s of the Eu^{3+} -complex. The membrane sensor with advantages of a long response range (2–7) and operational lifetime can apply for high throughput pH sensing. However, the sensor was still not suitable for alkaline solutions. Although the optical and luminescent pH sensors had made great progress in pH detection, they still face the difficult problems to work well in harsh environments, such as high temperature, high pressure, strong acid, strong alkali, etc.

Gas and vapor sensors

Gases are generated from industrial activities, volcanic eruptions, mining and burning of minerals. However, excessive toxic gases are seriously harmful for the health of animals and plants. For example, H_2S will damage human respiratory and nerve systems, resulting in unconsciousness (Zhou et al. 2019). NO_2 is related to respiratory tract and may cause serious

diseases of bosom frowsty, difficulty breathing and asthma (Bhat and Pandey 2018). A high concentration of ammonia may bring lung swelling of humans and even death (Masoud et al. 2018). Excessive intake of ethanol vapor will cause irritation of nose, eyes and mucous membrane (Boyes et al. 2014). Therefore, it is very important and urgent to develop green, low cost, fast response, highly selective and sensitive of sensors to monitor toxic gases in environment and industrial processes. According to different physical, chemical and electronic mechanisms, gas sensors can be divided into semiconductor metal oxide sensors, electrochemical sensors, optical sensors, catalytic combustion sensors, etc. Semiconductor metal oxide materials have become the most promising gas sensors because of their low cost, convenient operation, fast response and high sensitivity for target gases detection (Balasubramani 2020). Besides, electrochemical gas sensors work with the measured gas and then output the electrical signal proportional to the gas concentrations. Similarly, electrochemical sensors have the advantages of accuracy, reliability, rapidity and high sensitivity (Wang et al. 2020a, b). However, the optical sensors are based on the reactions between the measured gas and the sensitive layer, which result in changes of absorbance, fluorescence and color (Lochbaum et al. 2020).

The introduction of copper oxide nanoparticles (CuO NPs) with large specific surface and more reactive sites can improve the chemical reactivity and sensitivity of metal oxide semiconducting polymer membranes for gas sensing (Tanvir et al. 2016). Saleh t. Mahmoud and co-workers reported a novel semiconductor membrane sandwiched between a pair of electrodes for H₂S sensing, which was prepared by CuO NPs (via a colloid microwave-assisted hydrothermal method) and sodium carboxymethyl cellulose (CMC) powder with glycerol ionic liquid (5%) through the solution casting method (Hittini et al. 2020). When the optimum concentration of CuO was 5%, the nanoparticles were uniformly distributed in the membrane and no agglomeration. According to the change of electric current, the sensor was response to H₂S concentrations. Moreover, this sensor presented a decent selectivity towards H₂S in the presence of interfering gases (e.g. C₂H₄ and H₂), and a detection limit 15 ppm at a low temperature (40 °C). In addition, this membrane demonstrated a reversible behavior and low humidity dependence. The adsorption and

desorption of oxygen molecules can be used to explain the sensing mechanism of the membrane. These results suggested that the membrane provided a reliable sensing platform for H₂S detection in harsh environments, such as highly humid and low temperature. Another semiconductor thin film sensor was reported by Estefanía Núñez-Carmona and coworkers based on bacterial cellulose and zinc oxide (ZnO) (Núñez-Carmona et al. 2019). The best response of this sensor for detecting NO₂ was obtained. However, this sensor needed the activation of UV lamp, which was not beneficial to be widely used in practical applications.

Graphene oxide (GO) has relatively strong absorption properties of gas molecules, which is attributed to the characteristics of basal surfaces and prismatic edges. Besides, GO has a low permeability of most gases, which is expected to be an effective additive into cellulose-based solid electrolyte for regulating gas permeation. A green solid electrolyte based on functionalized cellulose/GO membrane was developed by Chen Zhongwei and co-workers, as an electrochemical gas sensor for alcohol vapor detection (Zhang et al. 2017). A schematic diagram of an alcohol fuel cell sensor (AFCS) and its electrochemical principle was shown in Fig. 7a. The concentration information of input ethanol vapor can be obtained by collecting the transferred electrons from anode to cathode as electrical signals. This sensor presented excellent selectivity towards ethanol vapor over water and acetone, with a low detection limit 25 ppm. Moreover, due to assist protons to move and through the membrane plane, a high water uptake of this cellulose/GO membrane offered promising ionic conductivity. The cellulose/GO membrane was used as an ideal electrochemical device for monitoring ethanol vapor in future practical applications.

Amino acid ionic liquids (AAIL) are green solvents for dissolving cellulose, which can act as the adsorption medium of gas (Uehara et al. 2019). A cellulose acetate membrane modified with a kind of amino acid ionic liquid (ProIL) through the phase inversion method, was designed by Kamatchi Sankaranarayanan and co-workers as an ammonia sensor (Mehta et al. 2020). ProIL was prepared by amino acids L-Proline and IL EMIM OH (base) via the neutralisation method. The sensing of ammonia by this membrane CA-ProIL was mainly based on the change in resistance, which was primarily due to chemisorption

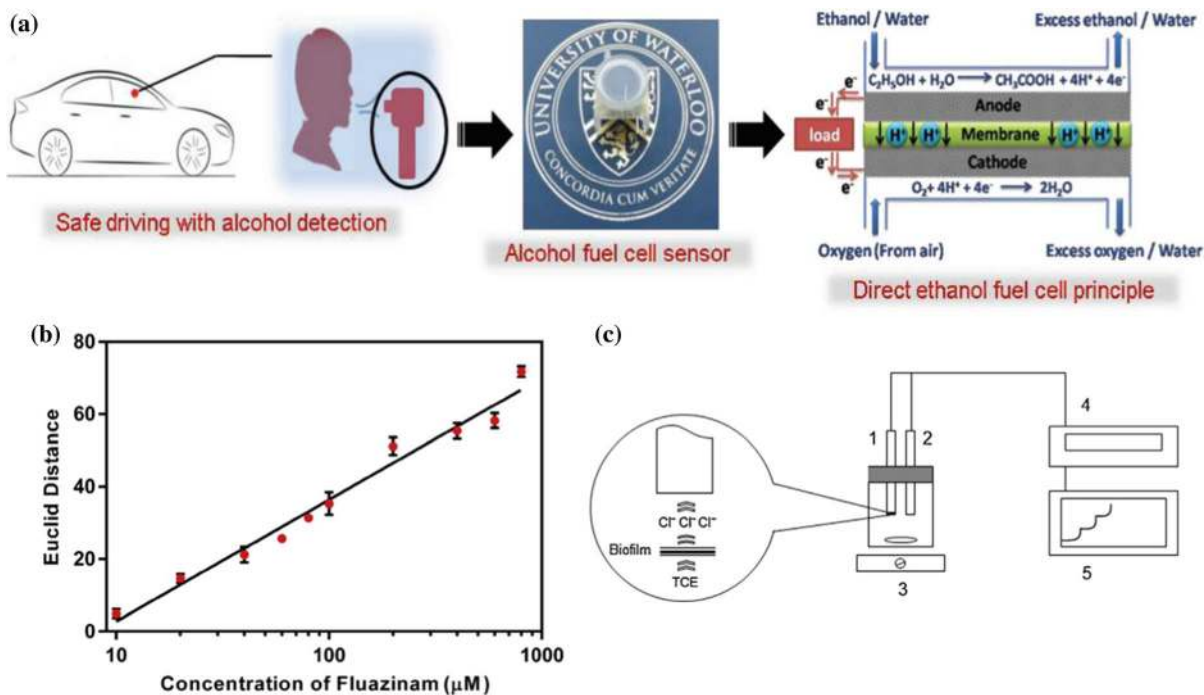


Fig. 7 **a** Schematic diagram of an AFCS and its electrochemical principle. Adapted with permission from Zhang et al. (2017), Copyright 2017, Wiley-VCH Verlag GmbH & Co. KGaA. **b** The linear equation between the euclidean distance and fluazinam concentrations. Adapted with permission from

Wang et al. (2020b), Copyright 2020, Elsevier B.V. **c** Schematic representation of the TCE biosensor assembly. (1) a working electrode, (2) a reference electrode, (3) a stirrer, (4) an ion meter, and (5) a recorder. Adapted with permission from Chee (2016), Copyright 2016, Elsevier B.V.

between ammonia and the surface of membrane. When acetone, ethanol and toluene existed, CA-ProIL showed a high selectivity for ammonia sensing with a low detection value 1 ppm at room temperature. The possible mechanism of adduct formation between ammonia and ProIL had been proved by Nuclear Magnetic Resonance (NMR) spectroscopy. Response time (60 s) and recovery time (78 s) suggested that this membrane CA-ProIL provided a potential for ammonia sensing in the future industrial areas.

Toxic organic compounds sensors

Pesticides, organic solvents and dyes are toxic and non-degradable. Their unreasonable use and arbitrary discharge would bring serious threats to soil, water, environment and even humans. Therefore, it is very important to develop green, simple, efficient and low-cost sensors for detecting toxic organic compounds instead of the traditional instrument methods.

Low concentration of fluazinam can be used as fungicide to control phytophthora blight (Bakirci et al.

2014). However, the excess use of fluazinam not only poses a serious threat to environment and food safety, but also reduces the soil quality and destroys the balance of biological population (Feng et al. 2015). MoS_2 QDs have the advantages of low toxicity and high stability, so they can be served as convenient, fast and efficient probes in the sensing fields (Wang et al. 2017; Lu et al. 2017). A cellulose membrane cross-linking MoS_2 QDs was developed by Hou Changjun and co-workers, which realized naked-eye and digital readout for detecting fluazinam in vegetable samples (Wang et al. 2020a, b). An overlapping between the absorption peak (347 nm) of fluazinam and the excitation (322 nm) of MoS_2 QDs caused inner filter effect (IFE), which led to the fluorescence quenching of the MoS_2 QDs. Thus, this sensor showed a highly selective for fluazinam rather than other similar pesticides, such as omethoate, glyphosate, triadimefon, etc. According to the linear equation between euclidean distance of ΔRGB and the logarithm of fluazinam concentration (10–800 μM), the detection limit 2.26 μM was obtained (Fig. 7b). In addition, π - π

stacking, hydrogen bond and electrostatic interaction of fluzinam with MoS₂ QDs can improve its selectivity and sensitivity. This proposed platform offered a convenient and efficient approach for fluazinam detection in agriculture and food safety.

Trichloroethylene (TCE) is widely acted as a cleansing agent for electronic parts. However, TCE is seriously harmful for soil and groundwater because of its unreasonable use and leakage. More importantly, TCE can cause serious impairment in the central nervous system when humans expose to a high level. Therefore, it inspires many researchers to develop simple and fast methods for TCE detection. Some studies have shown that an aerobic bacterium of *Pseudomonas sp.* strain ASA86 can be applied for TCE degradation (Chee 2011). A novel microbial biosensor based on *Pseudomonas sp.* strain ASA86 was designed by Gab-Joo Chee, utilizing a porous cellulose nitrate membrane with a chloride ion electrode to detect TCE (Chee 2016). After degradation of TCE by bacterium in the biosensor, chloride ions would be released, which can be detected by the ion electrode and output signal then converted into TCE value (Fig. 7c). This biosensor demonstrated a higher selectivity towards TCE than that of other organic solvents, such as 1,1-dichloroethylene, 1,2-dichloroethylene and 1,2-dichloroethane, etc. A good linear relationship of biosensor response with TCE concentrations (0.05–4 mg/L) was achieved with a detection limit 0.05 mg/L, which was lower than the TCE limit of industrial water and waste water stipulated by Japan. When the biosensor was at optimum conditions of pH 8.0 and 30 °C, the response time was about 5 min. However, the detection limit 0.05 mg/L of this biosensor was still higher than the limit value 0.03 mg/L of drinking water standard. Besides, toluene was used in culture medium of bacterium, which left a potential threat to the environment.

Because of its toxicity, mutagenicity, carcinogenicity and non-biodegradable, Methylene blue (MB) derived from dye industries is harmful to environment and humans (Auerbach et al. 2010; Hassan et al. 2014). However, the traditional UV–vis spectrometer for measuring MB is not suitable for on-site and convenient detection. Xu Xiaoping and co-workers reported a nitrated cellulose acetate (NCA) microfiltration membrane through phase inversion method, as a visual sensor for MB detection in tap water (He et al. 2016). In the filtration process of trace MB with

this membrane, MB molecules can be concentrated on the membrane to achieve a visual response. The membrane displayed a highly selective for MB detection, which was not influenced by bromophenol blue and crystal violet. When the membrane filtered 30 mL, the naked-eye detection limit 0.001 mg/L was achieved. Although the membrane sensor realized the portable detection of MB, it needed a large volume of solution.

Biosensors

Biomolecular sensors

Realizing the efficient detection of biological molecules in organisms is very important for disease prevention, clinical medicine and other processes. Glucose is widely distributed in human blood, urine, tears, etc. Therefore, glucose needs to be detected in time for preventing a high level, which leads to diabetes. A cellulose-based strips (CBS) was designed by Luo Xiaogang and co-workers, through oxidized cellulose membranes and glucose oxidase (GO_x)/horseradish peroxidase (HRP) via schiff-base reaction (Luo et al. 2019). CBS can be used as enzyme colorimetric assay for fast (within 5 min), sensitive and naked-eye detection of glucose. A schematic diagram of the preparation of CBS and detection of glucose was shown in Fig. 8a. The sensing mechanism was briefly described as follows: first, GO_x can catalyze the oxidation of glucose to form H₂O₂ by molecular oxygen. An obvious blue color was observed by the reaction of H₂O₂ with 3,3',5,5'-tetramethylbenzidine (TMB) under the oxidation of HRP. CBS presented a highly selective for glucose in presence of other carbohydrates (e.g. lactose, fructose, sucrose and maltose). A good linear relationship between the color intensity (recorded by a simple camera) and glucose concentrations (1–11 mM) was obtained with a detection limit (0.45 mM), which met the normal detection parameter 3.9–6.4 mM of glucose in human serum. In all, CBS provided a semi-quantitative approach for glucose detection in areas of biosensors, drug carriers and biomedicine.

Interleukin-6 (IL-6) is a pleiotropic cytokine, which plays an important role in immunity, tissue repair and metabolism, etc. Due to various disadvantages of large sample volume, long incubation time and complicated

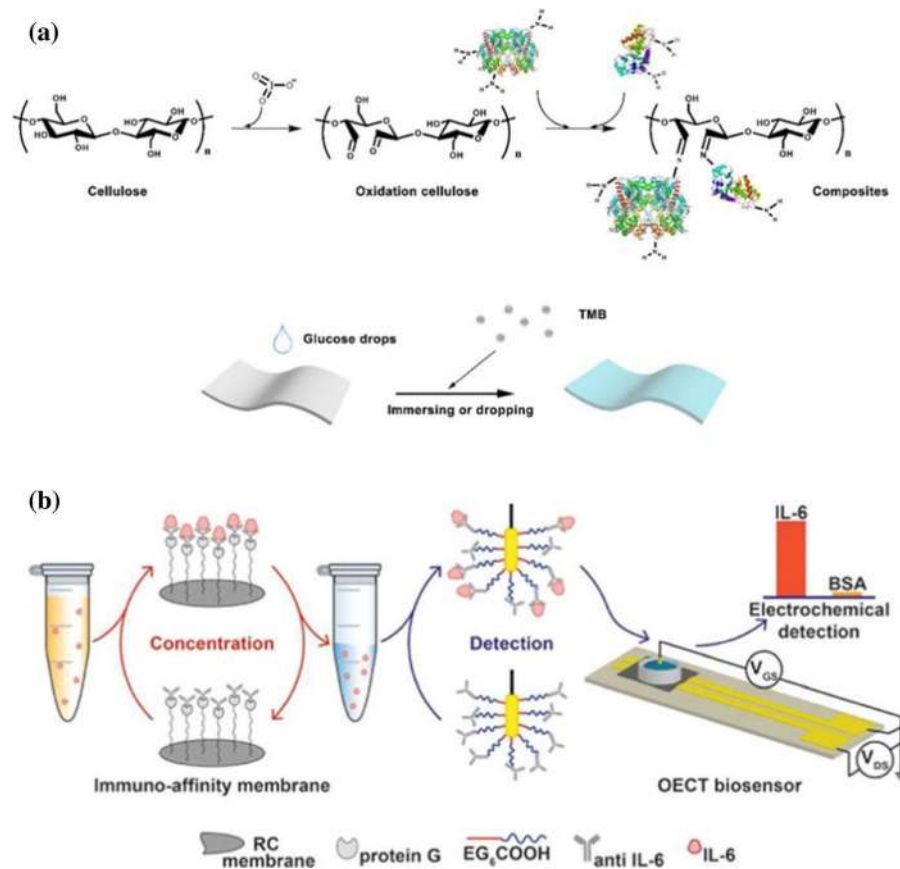


Fig. 8 **a** The preparation process of the cellulose-based strips and their glucose detection. Adapted with permission from Luo et al. (2019), Copyright 2019, American Chemical Society. **b** Schematic illustration of the selective concentration and

electrochemical detection of IL-6. Adapted with permission from Gentili et al. (2018), Copyright 2018, Royal Society of Chemistry

sample labelling process, the most common method of enzyme-linked immunosorbent assay (ELISA) is not suitable for real-time or dynamic monitoring of cytokine (Liu et al. 2016). However, the minimizing costs and processing time of label-free approaches can be applied for direct detection of antibody-antigen (Ab–Ag) recognition events. Besides, organic electrochemical transistors (OECTs) have the advantages of tissue compatibility, high stability and efficient operation, which can be acted as chemical sensors and biosensors (Lin and Yan 2012; Liao et al. 2015; Tang et al. 2011). A label-free and selective approach of IL-6 detection was prepared by Denis Gentili and co-workers, through combining an OECT with an immuno-affinity regenerated cellulose membrane (Gentili et al. 2018). The OECT gate electrode can be modified by an oligo (ethylene glycol)-terminated

self-assembled alkanethiolate monolayer (SAM), which can immobilize anti IL-6 antibodies and inhibit non-specific biomolecule binding. Figure 8b displayed the schematic diagram of selective concentration and electrochemical detection of IL-6. Antibody-antigen (Ab–Ag) molecular recognition events occurred in the preconcentrated IL-6 and anti IL-6 antibodies on the OECT gate electrode, which was converted into physically detectable signals. The preconcentration step of the immune-affinity membrane promoted IL-6 detection in physiological concentration. In addition, a detection limit of IL-6 was raised to 220 pg/mL.

Plasmodium falciparum histidine-rich protein 2 (PfHRP2) level in whole blood samples can be used as a parameter for diagnosing *P. falciparum* infection (Hendriksen et al. 2013). Similarly, a wash-free and

label-free immunoassay technique was developed by Peter B. Lillehoj for rapid electrochemical detection of *Pf*HRP2 in whole blood samples (Dutta and Lillehoj 2018). A unique detection method was based on electrochemical-chemical (EC) redox cycling with an affinity-based protein quantification strategy for signal amplification. The detection of *Pf*HRP2 with this immunoassay sensor would not be interfered by other electroactive species (e.g. glucose, uric acid and ascorbic acid). Moreover, a detection range (100 ng/mL–100 µg/mL) of *Pf*HRP2 concentrations was obtained, which encompassed the clinically relevant level of *P. falciparum* infection. This immunoassay offered a label-free and real-time method for proteins electrochemical detection in biomedical applications.

Urea content in biological urine is an important index in clinical diagnosis. A biosensor based on oxazine 170 perchlorate (O17)-ethyl cellulose (EC) membrane immobilized urease was prepared by Jong Il Rhee for ratiometric fluorescent detection of urea (Dinh Duong and Il Rhee 2015). Under the catalysis of the urease, urea will hydrolyze to produce ammonia, which can react with O17 to cause the change of two fluorescence emission intensities ($\lambda_{em} = 630$ nm and $\lambda_{em} = 565$ nm). According to a linear relationship between the ratio I_{565}/I_{630} of the fluorescence intensities and urea concentrations, a detection range 0.01–0.1 M with LOD of 0.027 mM and a detection range 0.1–1.0 M with LOD of 0.224 mM were obtained. Moreover, after 266 tests in two months, the membrane biosensor still had a good sensitivity, which suggested that this membrane had long-term stability. The biosensor supplied a potential method for urea-sensing in food safety and clinical diagnostics. Similarly, a ratiometric fluorescent biosensor for L-arginine (Arg) and L-asparagine (Asn) detection was designed by Jong Il Rhee, which was combined oxazine 170 perchlorate (O17)-ethyl cellulose (EC) membrane with enzymes and hydrogel polyurethane (An et al. 2017). Ammonium ions were produced by the hydrolysis reactions of urea and L-Arg under the catalysis of the urease and arginase, as well as the hydrolysis reaction of L-Asn under the catalysis of asparaginase. Ammonium ions can react with O17, which led to the ratio I_{565}/I_{630} change of the fluorescence intensities, and its proportional to L-Arg and L-Asn concentrations. A concentration range (0.1–10 mM) of L-Arg or L-Asn detection was achieved. The development of this biosensor offered

a simple and sensitive method for L-Arg and L-Asn determination in biological fluids, drugs and foods.

Enantiomers of chiral substances are very important in drug discovery and pharmaceutical industry, thus it is urgent to develop a simple, rapid and sensitive method for detecting of chiral molecules. Erhan Zor and co-workers reported a lab-in-a-syringe (LIS) device for colorimetric enantioselective of chiral species sensing, which was consisted of AuNPs-loaded cellulose acetate membrane (CAM) as the conjugate pad and non-loaded CAM as detection pad (Zor and Bekar 2017). The conjugate pad was used to capture analytes, which can be recognized by the detection pad and signalled for the captured analytes. Aggregation of AuNPs was caused by the enantioselective interaction between the inherently chiral AuNPs and enantiomers, and subsequently led to a distinct colour change from red to purple within 5 min. There existed a linear equation between colour intensity and L-Alanine concentrations (1–5 mM), with LOD of 0.77 mM. On the contrary, D-Alanine did not cause color changes and was not selectively detected. This lab-in-a-syringe (LIS) device paved a novel enantiosensing way for chiral molecules in biomedical fields and pharmaceutical industry.

Pathogen sensors

Due to environmental changes, species diversity and large-scale use of antibiotics, various pathogens caused the breaking out of infectious diseases, such as Ebola virus, avian influenza virus, swine influenza virus and COVID-19. The traditional pathogen detection methods have the disadvantages of complex experimental operation, high requirements for environment and personnel, which are difficult to meet the needs of rapid detection of pathogens.

When analytes are adsorbed on the substrate surface, Surface enhanced Raman scattering (SERS) can generate enhanced Raman signals, which can be used as biosensors (Pieczonka and Aroca 2008). Vladimir V. Tsukruk and co-workers reported a novel SERS substrate based on cellulose nanofibers (CNFs) membrane and gold nanorods (AuNRs) via direct vacuum-assisted filtration method for simultaneous detection of *Escherichia coli* and rhodamine 6G (R6G) (Zhang et al. 2018). The nanoporous morphology of CNFs matrix was contributed to the filtration, retention and preconcentration of analytes for

enhancing SERS performance. Besides, the plasmonic CNFs membranes had various excellent optical properties, including high transmission in the vis-NIR range, low scattering, almost no fluorescence and Raman background, which were applicable to the SERS detection. More interesting, the AuNR/CNF membrane can realize dual operational modes at two excitation wavelengths (532 nm and 785 nm). When the longer excitation wavelength was at 785 nm, the AuNR/CNF membrane displayed autofluorescence suppression for better detecting *Escherichia coli* with only 100–200 s integration time instead of hours of traditional Raman required. A better Raman scattering efficiency was generated by the shorter excitation wavelength (532 nm) to recognize R6G dyes, with a detection limit down to 10 pM. Although this SERS approach provided sensitive and fast performances, it required a Raman spectrometer.

Pathogenic *Escherichia coli* O157:H7 is related to bloody diarrhea, abdominal cramps, hemolytic uremic syndrome, renal failure and even death (Richard and Laura 2005). One of the most commonly immunological methods for detecting pathogens is the sandwich ELISA (enzyme-linked immunosorbent assay). A novel chitosan/cellulose nanocrystals/glycerol membrane immobilized monoclonal anti-Shiga toxin 2B antibody (mAnti-stx2B-Ab) with the indirect ELISA method was developed by Monique Lacroix and co-workers, for simple and sensitive detection of *Escherichia coli* O157:H7 (Shankar et al. 2020). A combination of the high specific surface area of the CNCs and functional amino units of the chitosan can result in the increase of antibodies immobilization on membrane surface. Besides, glycerol can not only be served as the membrane stabilizer, but also improved the flexibility of the membranes. The results showed that CNCs concentrations and chitosan parameters of higher molecular weight, deacetylation degree and viscosity had an important impact on the signal of detection. A detection limit 1 log CFU/mL of *Escherichia coli* O157:H7 was obtained by this immunological membrane. However, compared with the traditional methods of 24 h, the needed time of *Escherichia coli* O157:H7 detection by this novel method was only 4 h. Monique Lacroix reported a novel spider web trap approach (SWTA) for simultaneous enrichment, capture and detection of *Escherichia coli* O157:H7 by indirect ELISA method, which was based on chitosan/cellulose nanocrystals/glycerol

nanocomposite membrane (Baraketi et al. 2020). The introduction of CNCs into this nanocomposite membrane can improve the capture of the protein and the detection signal of the pathogen. Moreover, compared with traditional methods, the innovative SWTA did not need any sample preparation, which could minimize the risks of cross-contamination. The development of this CNC-based membrane with indirect ELISA method offered a convenient and sensitive strategy for *Escherichia coli* O157:H7 detection in food industries and drinking waters.

As an in vitro diagnostic technique, Lateral flow assays (LFAs) can be widely used in disease diagnosis, food detection and environment monitoring because of their low-cost, convenient, portable and efficient, etc. (Geertruida et al. 2009). Quantum dots (QDs) and graphene oxide (GO) exhibited excellent photo-physical properties, which had been intensely applied in biosensing areas (Park et al. 2017; Morales-Narvaez and Merkoci 2019). A lateral flow immunoassay for highly sensitive detection of *Escherichia coli* O157:H7 was developed by Arben Merkoçi and co-workers, with QDs printing on nitrocellulose membrane substrate as control line and antibody-decorated QDs on the same substrate as test line (Narváez et al. 2015). Upon excitation, when there was no pathogen, the fluorescence of the control line and test line was quenched by a GO flow. However, when the test line selectively captured the pathogens, it did not be significantly quenched compared to the control line (Fig. 9a). The quenching ratio Q_{TL}/Q_{CL} of the test line and control line determined the selectivity and sensitivity of this lateral flow immunoassay. This sensitive of this detection method for *Escherichia coli* O157:H7 was clearly observed to 10 CFU/mL in standard buffer and 100 CFU/mL in bottled water and milk, respectively. However, the performance of this lateral flow test was affected by the changes of the sample matrix and microenvironments, such as polarity, viscosity, pH and ionic strength, etc. *Staphylococcus aureus*, as a common clinical pathogen, can cause skin purulent infection, pneumonia, pericarditis, sepsis and other diseases (Tong et al. 2015). Our group reported the lateral flow assays based on nitrocellulose membranes with cellulose nanofibers for the determination of *Staphylococcus aureus* (Tang et al. 2019) (Fig. 9b–d). The results showed that the incorporation of cellulose nanofibers into nitrocellulose membranes could improve the adsorption capacity of biomolecules on

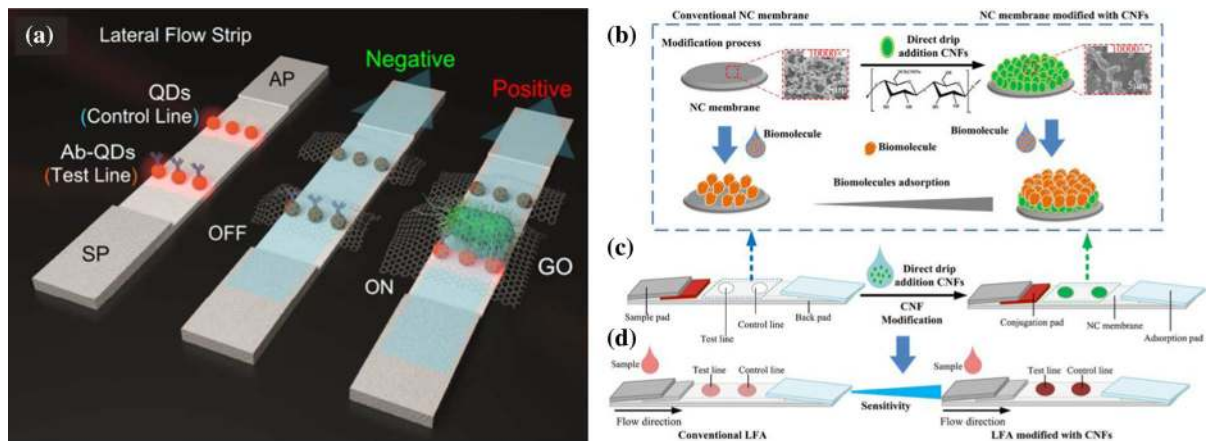


Fig. 9 **a** Schematic representation of photoluminescent lateral flow test revealed by graphene oxide (GO) for pathogen detection. Adapted with permission from Narváez et al. (2015), Copyright 2015, American Chemical Society. Schematic illustration of LFAs test strip modified with CNFs. **b** The

membrane substrate, which was related to the changes of the pore size, porosity, surface groups and surface area of these membranes. According to the changes of the color signal of test line, a detection limit 0.05 nM of cellulose nanofibers-modified LFAs was considerably lower than that of unmodified LFAs at 1 nM, which indicated that the sensitivity of this modified-LFAs for *Staphylococcus aureus* detection could be increased 20-fold by adding cellulose nanofibers into the original nitrocellulose membranes. These LFAs provided fast, low-cost, easy to operate and sensitive techniques for pathogen detection in disease diagnosis, food safety and environmental monitoring.

Conclusions

In this article, we reviewed the preparations of cellulose membranes and their latest developments in the fields of pressure/strain, temperature, humidity, metal cations, non-metal ions, pH, gas/vapor, toxic organic compounds, biomolecules, pathogens and other sensing applications. Combining metal nanowires, metal nanoparticles, graphene oxide/reduced graphene oxide, carbon dots, quantum dots, carbon nanotubes, fluorophores, organic dyes and antigen-antibodies with cellulose membranes via physical and chemical bonding can show excellent sensing performances, which indicate that cellulose membranes have

great momentums and broad application prospects in the sensing fields. However, there are still some problems: (1) Inherent technical bottlenecks of detection selectivity, sensitivity, response time and reversibility in the sensing fields are still existed. (2) The long-term stability of cellulose membranes in harsh environments (e.g. strong acid, strong alkali, strong solvent, high temperature, high pressure, high ionic strength) still needs to be considered. (3) Cellulose membrane-based sensors for achieving multi-functional simultaneously detection had rarely been reported. (4) The sensing response mechanisms of cellulose membranes are still unclear. And based on the theoretical design, the relationship between the structures and properties of cellulose membranes should be explored. (5) Although a large number of cellulose sensing membranes have been developed, few of them can be commercialized. In addition, low cost, recyclable, portable, biocompatible, miniaturized, integrated and intelligent properties for future practical applications need greater improvement. Moreover, more new applications of cellulose sensing membranes in other fields and interdisciplinary fields should also be explored. With continuous efforts to face these challenges of cellulose membrane-based sensors, we firmly believe that although the road ahead is tortuous, the future is bright.

Acknowledgments The authors thank the Key scientific research plan (Key Laboratory) of Shaanxi Provincial

Education Department (No. 17JS016), and the International Joint Research Center for biomass chemistry and materials, Shaanxi international science and technology cooperation base (2018GHJD-19), and Shaanxi Key industry innovation chain projects (2020ZDLGY11-03), and Science and Technology Plan of Weiyang District of Xi'an (201910) for financial support.

References

- Amin AS (2015) Application of a triacetylcellulose membrane with immobilized of 5-(2',4'-dimethylphenylazo)-6-hydroxypyrimidine-2,4-dione for mercury determination in real samples. *Sens Actuators B* 221:1342–1347. <https://doi.org/10.1016/j.snb.2015.07.106>
- Amin AS, Ahmed IS (2010) Complexation and spectrophotometric study of samarium(III) using pyrimidine Azo derivatives in the presence of cetyltrimethyl ammonium bromide. *Anal Lett* 43:2598–2608. <https://doi.org/10.1080/00032711003726910>
- An K, Duong HD, Rhee JI (2017) Ratiometric fluorescent L-arginine and L-asparagine biosensors based on theoxazine 170 perchlorate-ethyl cellulose membrane. *Eng Life Sci* 17:847–856. <https://doi.org/10.1002/elsc.201700033>
- Angst U, Elsener B, Larsen CK, Vennesland Ø (2009) Critical chloride content in reinforced concrete—a review. *Cem Concr Res* 39:1122–1138. <https://doi.org/10.1016/j.cemconres.2009.08.006>
- Auerbach SS, Bristol DW, Peckham JC, Travlos GS, Hebert CD, Chhabra RS (2010) Toxicity and carcinogenicity studies of methylene blue trihydrate in F344N rats and B6C3F1 mice. *Food Chem Toxicol* 48:169–177. <https://doi.org/10.1016/j.fct.2009.09.034>
- Bakirci GT, Yaman Acay DB, Bakirci F, Otles S (2014) Pesticide residues in fruits and vegetables from the Aegean region, Turkey. *Food Chem* 160:379–392. <https://doi.org/10.1016/j.foodchem.2014.02.051>
- Balasubramani V (2020) Review—recent advances in electrochemical impedance spectroscopy based toxic gas sensor using semiconducting metal oxides. *J Electrochem Soc* 167:037572. <https://doi.org/10.1149/1945-7111/ab77a0>
- Baraketi A, D'Auria S, Shankar S, Fracchini C, Salmieri S, Menissier J, Lacroix M (2020) Novel spider web trap approach based on chitosan/cellulose nanocrystals/glycerol membrane for the detection of *Escherichia coli* O157:H7 on food surfaces. *Int J Biol Macromol* 146:1009–1014. <https://doi.org/10.1016/j.ijbiomac.2019.09.225>
- Bassouini M, Abdel-Aziz MH, Zoromba MS, Abdel-Hamid SMS, Drioli E (2019) A review of polymeric nanocomposite membranes for water purification. *J Ind Eng Chem* 73:19–46. <https://doi.org/10.1016/j.jiec.2019.01.045>
- Bethke K et al (2018) Functionalized cellulose for water purification, antimicrobial applications, and sensors. *Adv Funct Mater* 28:1800409. <https://doi.org/10.1002/adfm.201800409>
- Bhat M, Pandey A (2018) Estimation of NO₂, SO₂ and its impact on respiratory human health. *Res J Chem Environ Sci* 6:90–98
- Blank TA, Eksperiandova LP, Belikov KN (2016) Recent trends of ceramic humidity sensors development: a review. *Sens Actuators B* 228:416–442. <https://doi.org/10.1016/j.snb.2016.01.015>
- Boyes WK, Degn LL, Martin SA, Lyke DF, Hamm CW, Herr DW (2014) Neurophysiological assessment of auditory, peripheral nerve, somatosensory, and visual system functions after developmental exposure to ethanol vapors. *Neurotoxicol Teratol* 43:1–10. <https://doi.org/10.1016/j.ntt.2014.02.006>
- Chamkouri N (2015) Development of long-term optical pH sensor using phenol red based on triacetylcellulose membranes. *Int J Pharm Technol* 7:9096–9104
- Chee GJ (2011) Biodegradation analyses of trichloroethylene (TCE) by bacteria and its use for biosensing of TCE. *Talanta* 85:1778–1782. <https://doi.org/10.1016/j.talanta.2011.07.002>
- Chee GJ (2016) A novel whole-cell biosensor for the determination of trichloroethylene. *Sens Actuators B* 237:836–840. <https://doi.org/10.1016/j.snb.2016.07.034>
- Chu CY, Tung L, Lin CY (2013) Effect of substrate concentration and pH on biohydrogen production kinetics from food industry wastewater by mixed culture. *Int J Hydrog Energy* 38:15849–15855. <https://doi.org/10.1016/j.ijhydene.2013.07.088>
- Dai L, Wang Y, Zou X, Chen Z, Liu H, Ni Y (2020) Ultrasensitive physical, bio, and chemical sensors derived from 1-, 2-, and 3-D nanocellulosic materials. *Small* 16:1906567. <https://doi.org/10.1002/smll.201906567>
- Dinh Duong H, Il Rhee J (2015) Development of a ratiometric fluorescent urea biosensor based on the urease immobilized onto the oxazine 170 perchlorate-ethyl cellulose membrane. *Talanta* 134:333–339. <https://doi.org/10.1016/j.talanta.2014.10.064>
- Douglass EF, Avci H, Boy R, Rojas OJ, Kotek R (2017) A review of cellulose and cellulose blends for preparation of bio-derived and conventional membranes, nanostructured thin films, and composites. *Polym Rev* 58:102–163. <https://doi.org/10.1080/15583724.2016.1269124>
- Duong HD, Kim HL, Rhee JI (2018) Development of colorimetric and ratiometric fluorescence membranes for detection of nitrate in the presence of aluminum-containing compounds. *Sensors*. <https://doi.org/10.3390/s18092883>
- Dutta G, Lillehoj PB (2018) Wash-free, label-free immunoassay for rapid electrochemical detection of PfHRP2 in whole blood samples. *Sci Rep* 8:17129. <https://doi.org/10.1038/s41598-018-35471-8>
- Elmizadeh H, Soleimani M, Faridbod F, Bardajee GR (2017) Ligand-capped CdTe quantum dots as a fluorescent nanosensor for detection of copper ions in environmental water sample. *J Fluoresc* 27:2323–2333. <https://doi.org/10.1007/s10895-017-2174-3>
- Fan J, Zhang S, Li F, Shi J (2020a) Cellulose-based sensors for metal ions detection. *Cellulose*. <https://doi.org/10.1007/s10570-020-03158-x>
- Fan J, Zhang S, Xu Y, Wei N, Wan B, Qian L, Liu Y (2020b) Apolyethylenimine/salicylaldehyde modified cellulose Schiff base for selective and sensitive Fe³⁺ detection. *Carbohydr Polym* 228:115379. <https://doi.org/10.1016/j.carbpol.2019.115379>

- Feng X, Wang K, Mu Z, Zhao Y, Zhang H (2015) Fluazinam-residue and dissipation in potato tubers and vines, and in field soil. *Am J Potato Res* 92:567–572. <https://doi.org/10.1007/s12230-015-9469-1>
- Fu W et al (2019) Electronic textiles based on aligned electrospun belt-like cellulose acetate nanofibers and graphene sheets: portable, scalable and eco-friendly strain sensor. *Nanotechnology* 30:045602. <https://doi.org/10.1088/1361-6528/aaed99>
- Geertruida A, Posthuma T, Jakob K, Aart A (2009) Lateral flow (immuno) assay: its strengths, weaknesses, opportunities and threats. A literature survey. *Anal Bioanal Chem* 393:569–582. <https://doi.org/10.1007/s00216-008-2287-2>
- Gentili D et al (2018) Integration of organic electrochemical transistors and immuno-affinity membranes for label-free detection of interleukin-6 in the physiological concentration range through antibody–antigen recognition. *J Mater Chem B* 6:5400–5406. <https://doi.org/10.1039/c8tb01697f>
- Ghoneim MT, Nguyen A, Dereje N, Huang J, Moore GC, Murzynowski PJ, Dagdeviren C (2019) Recent progress in electrochemical pH-sensing materials and configurations for biomedical applications. *Chem Rev* 119:5248–5297. <https://doi.org/10.1021/acs.chemrev.8b00655>
- Gotor R, Ashokkumar P, Hecht M, Keil K, Rurack K (2017) Optical pH sensor covering the range from pH 0–14 compatible with mobile-device readout and based on a set of rationally designed indicator dyes. *Anal Chem* 89:8437–8444. <https://doi.org/10.1021/acs.analchem.7b01903>
- Gu Y, Wang M, Li G (2017) CNTs-anchored cellulose fluorescent nanofiber membranes as fluorescence sensor for Cu^{2+} and Cr^{3+} . *Anal Methods* 9:6044–6048. <https://doi.org/10.1039/C7AY01994G>
- Hao J, Han MJ, Meng X (2009) Preparation and evaluation of thiol-functionalized activated alumina for arsenite removal from water. *J Hazard Mater* 167:1215–1221. <https://doi.org/10.1016/j.jhazmat.2009.01.124>
- Hassan AF, Abdel-Mohsen AM, Fouda MM (2014) Comparative study of calcium alginate, activated carbon, and their composite beads on methylene blue adsorption. *Carbohydr Polym* 102:192–198. <https://doi.org/10.1016/j.carbpol.2013.10.104>
- He S, Fang H, Xu X (2016) Filtering absorption and visual detection of methylene blue by nitrated cellulose acetate membrane. *Korean J Chem Eng* 33:1472–1479. <https://doi.org/10.1007/s11814-015-0231-7>
- He K, Zhan X, Liu L, Ruan X, Wu Y (2020) Ratiometric fluorescent paper-based sensor based on CdTe quantum dots and graphite carbonitride hybrid for visual and rapid determination of $\text{Cu}^{(2+)}$ in drinks. *Photochem Photobiol.* <https://doi.org/10.1111/php.13271>
- Hendriksen IC et al (2013) Defining falciparum-malaria-attributable severe febrile illness in moderate-to-high transmission settings on the basis of plasma PfHRP2 concentration. *J Infect Dis* 207:351–361. <https://doi.org/10.1093/infdis/jis675>
- Hittini W, Abu-Hani AF, Reddy N, Mahmoud ST (2020) Cellulose-copper oxide hybrid nanocomposites membranes for H₂S gas detection at low temperatures. *Sci Rep* 10:2940. <https://doi.org/10.1038/s41598-020-60069-4>
- Jamroz E, Kocot K, Zawisza B, Talik E, Gagor A, Sitko R (2019) A green analytical method for ultratrace determination of hexavalent chromium ions based on micro-solid phase extraction using amino-silanized cellulose membranes. *Microchem J* 149:104060. <https://doi.org/10.1016/j.microc.2019.104060>
- Jheng LC, Hsiao CH, Ko WC, Hsu SL, Huang YL (2019) Conductive films based on sandwich structures of carbon nanotubes/silver nanowires for stretchable interconnects. *Nanotechnology* 30:235201. <https://doi.org/10.1088/1361-6528/ab0483>
- Jiang X, Xia J, Luo X (2020a) Simple, rapid, and highly sensitive colorimetric sensor strips from a porous cellulose membrane stained with Victoria blue B for efficient detection of trace Cd(II) in water. *ACS Sustain Chem Eng* 8:5184–5191. <https://doi.org/10.1021/acssuschemeng.9b07614>
- Jiang Y et al (2020b) Preparation of dual-emission polyurethane/carbon dots thermoresponsive composite films for colorimetric temperature sensing. *Carbon* 163:26–33. <https://doi.org/10.1016/j.carbon.2020.03.013>
- Khullar S, Singh S, Das P, Mandal SK (2019) Luminescent lanthanide-based probes for the detection of nitroaromatic compounds in water. *ACS Omega* 4:5283–5292. <https://doi.org/10.1021/acsomega.9b00223>
- Kim T, Bao C, Hausmann M, Siqueira G, Zimmermann T, Kim WS (2019) 3D printed disposable wireless ion sensors with biocompatible cellulose composites. *Adv Electron Mater* 5:1800778. <https://doi.org/10.1002/aelm.201800778>
- Koch M, Bowes G, Ross C, Zhang XH (2013) Climate change and ocean acidification effects on seagrasses and marine macroalgae. *Glob Change Biol* 19:103–132. <https://doi.org/10.1111/j.1365-2486.2012.02791.x>
- Kulkarni PS, Ramekar PV, Kulkarni SD (2018) An optical sensor for selenite determination in aqueous samples. *J Anal Sci Technol.* <https://doi.org/10.1186/s40543-018-0136-2>
- Lee WJ, Bao Y, Hu X, Lim T-T (2019) Hybrid catalytic ozonation–membrane filtration process with CeO_x and MnO_x impregnated catalytic ceramic membranes for micropollutants degradation. *Chem Eng J* 378:121670. <https://doi.org/10.1016/j.cej.2019.05.031>
- Li J et al (2017a) Detection of trace nickel ions with a colorimetric sensor based on indicator displacement mechanism. *Sens Actuators B* 241:1294–1302. <https://doi.org/10.1016/j.snb.2016.09.191>
- Li J, Wang X, Huo D, Hou C, Fa H, Yang M, Zhang L (2017b) Colorimetric measurement of Fe^{3+} using a functional paper-based sensor based on catalytic oxidation of gold nanoparticles. *Sens Actuators B* 242:1265–1271. <https://doi.org/10.1016/j.snb.2016.09.039>
- Li N et al (2017c) Facile synthesis of cellulose acetate ultrafiltration membrane with stimuli-responsiveness to pH and temperature using the additive of F127-b-PDMAEMA. *Chin J Chem* 35:1109–1116. <https://doi.org/10.1002/cjoc.201600820>
- Li M et al (2018) Fluorescence detection and removal of copper from water using a biobased and biodegradable 2D soft material. *Chem Commun* 54:184–187. <https://doi.org/10.1039/c7cc08035b>
- Liao C, Mak C, Zhang M, Chan HL, Yan F (2015) Flexible organic electrochemical transistors for highly selective

- enzyme biosensors and used for saliva testing. *Adv Mater* 27:676–681. <https://doi.org/10.1002/adma.201404378>
- Lin P, Yan F (2012) Organic thin-film transistors for chemical and biological sensing. *Adv Mater* 24:34–51. <https://doi.org/10.1002/adma.201103334>
- Liu G, Qi M, Hutchinson MR, Yang G, Goldys EM (2016) Recent advances in cytokine detection by immunosensing. *Biosens Bioelectron* 79:810–821. <https://doi.org/10.1016/j.bios.2016.01.020>
- Liu j et al (2020) Naphthalimide-containing coordination polymer with mechanoresponsive luminescence and excellent metal ion sensing properties. *Dalton Trans* 49:3174–3180. <https://doi.org/10.1039/C9DT04928B>
- Lochbaum A et al (2020) Compact mid-infrared gas sensing enabled by an all-metamaterial design. *Nano Lett*. <https://doi.org/10.1021/acs.nanolett.0c00483>
- Lou M, Abdalla I, Zhu M, Yu J, Li Z, Ding B (2020) Hierarchically rough structured and self-powered pressure sensor textile for motion sensing and pulse monitoring. *ACS Appl Mater Interfaces* 12:1597–1605. <https://doi.org/10.1021/acsami.9b19238>
- Lu Z, Chen X, Hu W (2017) A fluorescence aptasensor based on semiconductor quantum dots and MoS₂ nanosheets for ochratoxin A detection. *Sens Actuators B* 246:61–67. <https://doi.org/10.1016/j.snb.2017.02.062>
- Lukojko E, Talik E, Gagor A, Sitko R (2018) Highly selective determination of ultratrace inorganic arsenic species using novel functionalized miniaturized membranes. *Anal Chim Acta* 1008:57–65. <https://doi.org/10.1016/j.aca.2017.12.038>
- Luo X, Xia J, Jiang X, Yang M, Liu S (2019) Cellulose-based strips designed based on a sensitive enzyme colorimetric assay for the low concentration of glucose detection. *Anal Chem* 91:15461–15468. <https://doi.org/10.1021/acs.analchem.9b03180>
- Lv C et al (2019a) Recent advances in graphene-based humidity sensors. *Nanomaterials*. <https://doi.org/10.3390/nano9030422>
- Lv P et al (2019b) In situ 3D bacterial cellulose/nitrogen-doped graphene oxide quantum dot-based membrane fluorescent probes for aggregation-induced detection of iron ions. *Cellulose* 26:6073–6086. <https://doi.org/10.1007/s10570-019-02476-z>
- Masoud N et al (2018) Ventilatory disorders associated with occupational inhalation exposure to nitrogen trihydride (ammonia). *Ind Health* 56:427–435
- Mautner A (2020) Nanocellulose water treatment membranes and filters: a review. *Polym Int*. <https://doi.org/10.1002/pi.5993>
- Mazza MMA, Raymo FM (2019) Structural designs for ratio-metric temperature sensing with organic fluorophores. *J Mater Chem C* 7:5333–5342. <https://doi.org/10.1039/c9tc00993k>
- Mehta P, Vedachalam S, Sathyaraj G, Garai S, Arthana-reeswaran G, Sankaranarayanan K (2020) Fast sensing ammonia at room temperature with proline ionic liquid incorporated cellulose acetate membranes. *J Mol Liq* 305:112820. <https://doi.org/10.1016/j.molliq.2020.112820>
- Morales-Narvaez E, Merkoçi A (2019) Graphene oxide as an optical biosensing platform: a progress report. *Adv Mater* 31:1805043. <https://doi.org/10.1002/adma.201805043>
- Narvaez E, Naghdi T, Zor E, Merkoçi A (2015) Photoluminescent lateral-flow immunoassay revealed by graphene oxide: highly sensitive paper-based pathogen detection. *Anal Chem* 87:8573–8577. <https://doi.org/10.1021/acs.analchem.5b02383>
- Núñez-Carmona E, Bertuna A, Abbatangelo M, Sberveglieri V, Comini E, Sberveglieri G (2019) BC-MOS: the novel bacterial cellulose based MOS gas sensors. *Mater Lett* 237:69–71. <https://doi.org/10.1016/j.matlet.2018.11.011>
- Ning Y, Zhu M, Zhang J-L (2019) Near-infrared (NIR) lanthanide molecular probes for bioimaging and biosensing. *Coord Chem Rev* 399:213028. <https://doi.org/10.1016/j.ccr.2019.213028>
- Park M, Seo TS (2019) An integrated microfluidic device with solid-phase extraction and graphene oxide quantum dot array for highly sensitive and multiplex detection of trace metal ions. *Biosens Bioelectron* 126:405–411. <https://doi.org/10.1016/j.bios.2018.11.010>
- Park Y, Jeong S, Kim S (2017) Medically translatable quantum dots for biosensing and imaging. *J Photochem Photobiol C* 30:51–70. <https://doi.org/10.1016/j.jphotochemrev.2017.01.002>
- Pieczonka NP, Aroca RF (2008) Single molecule analysis by surface-enhanced Raman scattering. *Chem Soc Rev* 37:946–954. <https://doi.org/10.1039/b709739p>
- Qi HJ, Chen SH, Zhang ML, Shi H, Wang SQ (2010) DNA microarrays for visual detection of human pathogenic microorganisms based on tyramine signal amplification coupled with gold label silver stain. *Anal Bioanal Chem* 398:2745–2750. <https://doi.org/10.1007/s00216-010-4189-3>
- Rao A, Kumar GS, Roy S, Rajesh AT, Devatha G, Pillai PP (2019) Turn-on selectivity in inherently nonselective gold nanoparticles for Pb²⁺ detection by preferential breaking of interparticle interactions. *ACS Appl Nano Mater* 2:5625–5633. <https://doi.org/10.1021/acsanm.9b01168>
- Regev N, Wulch D (2019) Remote sensing of vital signs using an ultra-wide-band radar. *Int J Remote Sens* 40:6596–6606. <https://doi.org/10.1080/2150704x.2019.1573335>
- Richard L, Laura D (2005) *Escherichia coli* O157:H7 outbreak associated with consumption of ground beef, June–July 2002. *Public Health Rep* 120:174–178. <https://doi.org/10.1177/003335490512000211>
- Sadasivuni KK, Kafy A, Kim H-C, Ko H-U, Mun S, Kim J (2015) Reduced graphene oxide filled cellulose films for flexible temperature sensor application. *Synth Met* 206:154–161. <https://doi.org/10.1016/j.synthmet.2015.05.018>
- Shaheen K, Shah Z, Khan B, Adnan, Omer M, Alamzeb M, Suo H (2020) Electrical, photocatalytic, and humidity sensing applications of mixed metal oxide nanocomposites. *ACS Omega* 5:7271–7279. <https://doi.org/10.1021/acsomega.9b04074>
- Shankar S et al (2020) Development of support based on chitosan and cellulose nanocrystals for the immobilization of anti-Shiga toxin 2B antibody. *Carbohydr Polym* 232:115785. <https://doi.org/10.1016/j.carbpol.2019.115785>
- Syrový T et al (2019) Wide range humidity sensors printed on biocomposite films of cellulose nanofibril and

- poly(ethylene glycol). *J Appl Polym Sci*. <https://doi.org/10.1002/APP.47920>
- Tang J, Xu Z, Zhou L, Qin H, Wang Y, Wang H (2010) Rapid and simultaneous detection of *Ureaplasma parvum* and *Chlamydia trachomatis* antibodies based on visual protein microarray using gold nanoparticles and silver enhancement. *Diagn Microbiol Infect Dis* 67:122–128. <https://doi.org/10.1016/j.diagmicrobio.2010.01.009>
- Tang H, Yan F, Lin P, Xu J, Chan HLW (2011) Highly sensitive glucose biosensors based on organic electrochemical transistors using platinum gate electrodes modified with enzyme and nanomaterials. *Adv Funct Mater* 21:2264–2272. <https://doi.org/10.1002/adfm.201002117>
- Tang RH, Liu LN, Zhang SF, Li A, Li Z (2019) Modification of a nitrocellulose membrane with cellulose nanofibers for enhanced sensitivity of lateral flow assays: application to the determination of *Staphylococcus aureus*. *Mikrochim Acta* 186:831. <https://doi.org/10.1007/s00604-019-3970-z>
- Tanvir N, Yurchenko O, Wilbertz C, Urban G (2016) Investigation of CO₂ reaction with copper oxide nanoparticles for room temperature gas sensing. *J Mater Chem A* 4:5294–5302. <https://doi.org/10.1039/C5TA09089J>
- Thakur N, Kumar SA, Kumar KSA, Pandey AK, Kumar SD, Reddy AVR (2015) Development of a visual optode sensor for onsite determination of Hg(II). *Sens Actuators B* 211:346–353. <https://doi.org/10.1016/j.snb.2015.01.087>
- Thakur VK, Voicu SI (2016) Recent advances in cellulose and chitosan based membranes for water purification: a concise review. *Carbohydr Polym* 146:148–165. <https://doi.org/10.1016/j.carbpol.2016.03.030>
- Tong SY, Davis JS, Eichenberger E, Holland TL, Fowler VG Jr (2015) *Staphylococcus aureus* infections: epidemiology, pathophysiology, clinical manifestations, and management. *Clin Microbiol Rev* 28:603–661. <https://doi.org/10.1128/CMR.00134-14>
- Uehara Y, Karami D, Mahinpey N (2019) CO₂ adsorption using amino acid ionic liquid-impregnated mesoporous silica sorbents with different textural properties. *Microporous Mesoporous Mater* 278:378–386. <https://doi.org/10.1016/j.micromeso.2019.01.011>
- Ventura MG, Stibilj V, Freitas MdC, Pacheco AMG (2009) Determination of ultratrace levels of selenium in fruit and vegetable samples grown and consumed in Portugal. *Food Chem* 115:200–206. <https://doi.org/10.1016/j.foodchem.2008.10.089>
- Waleed Al-Qaysi W, Duerkop A (2018) A luminescent europium complex for wide-range pH sensors and sensor microtiter plates. *Analyst* 143:3176–3183. <https://doi.org/10.1039/c8an00775f>
- Wang CY, Fang BY, Yao MH, Zhao YD (2016a) Visualization detection of ultratrace lead and cadmium ions using cellulose acetate membrane based on silver stain. *Sens Actuators B* 228:643–648. <https://doi.org/10.1016/j.snb.2016a.01.080>
- Wang X, Li J-H, Li Y-L, Liu L-J, Guan W-M (2016b) Emulsion-templated fully three-dimensional interconnected porous titania ceramics with excellent humidity sensing properties. *Sens Actuators B* 237:894–898. <https://doi.org/10.1016/j.snb.2016.07.014>
- Wang X, Wu Q, Jiang K, Wang C, Zhang C (2017) One-step synthesis of water-soluble and highly fluorescent MoS₂ quantum dots for detection of hydrogen peroxide and glucose. *Sens Actuators B* 252:183–190. <https://doi.org/10.1016/j.snb.2017.05.177>
- Wang J et al (2020a) Stabilized zirconia-based solid state electrochemical gas sensor coupled with CdTiO₃ for acetylene detection. *Sens Actuators B* 316:128199. <https://doi.org/10.1016/j.snb.2020.128199>
- Wang X et al (2020b) MoS₂ QDs-based sensor for measurement of fluazinam with triple signal output. *Anal Chim Acta* 1108:152–159. <https://doi.org/10.1016/j.aca.2020.02.028>
- Weishaupt R et al (2020) Antibacterial, cytocompatible, sustainably sourced: cellulose membranes with bifunctional peptides for advanced wound dressings. *Adv Healthc Mater* 9:1901850. <https://doi.org/10.1002/adhm.201901850>
- Xiao W, Ding L, He J, Huang J (2019) Preparation of lucigenin-doped silica nanoparticles and their application in fiber optic chloride ion sensor. *Opt Mater* 98:109467. <https://doi.org/10.1016/j.optmat.2019.109467>
- Yang C, Veiga C, Rodriguez-Andina JJ, Farina J, Iniguez A, Yin S (2019) Using PPG signals and wearable devices for atrial fibrillation screening. *IEEE Trans Ind Electron* 66:8832–8842. <https://doi.org/10.1109/tie.2018.2889614>
- Ye X, Kang Y, Zhou J (2020) Rhodamine labeled cellulose nanocrystals as selective “naked-eye” colorimetric and fluorescence sensor for Hg²⁺ in aqueous solutions. *Cellulose*. <https://doi.org/10.1007/s10570-020-03126-5>
- Zhang J, Zhou L (2018) Preparation and optimization of optical pH sensor based on sol–gel. *Sensors*. <https://doi.org/10.3390/s18103195>
- Zhang J et al (2017) Green solid electrolyte with cofunctionalized nanocellulose/graphene oxide interpenetrating network for electrochemical gas sensors. *Small Methods* 1:1700237. <https://doi.org/10.1002/smt.201700237>
- Zhang S, Xiong R, Mahmoud MA, Quigley EN, Chang H, El-Sayed M, Tsukruk VV (2018) Dual-excitation nanocellulose plasmonic membranes for molecular and cellular SERS detection. *ACS Appl Mater Interfaces* 10:18380–18389. <https://doi.org/10.1021/acsami.8b04817>
- Zhang H, Sun X, Hubbe MA, Pal L (2019a) Highly conductive carbon nanotubes and flexible cellulose nanofibers composite membranes with semi-interpenetrating networks structure. *Carbohydr Polym* 222:115013. <https://doi.org/10.1016/j.carbpol.2019.115013>
- Zhang H, Zhao S, Wang X, Ren X, Ye J, Huang L, Xu S (2019b) The enhanced photoluminescence and temperature sensing performance in rare earth doped SrMoO₄ phosphors by aliovalent doping: from material design to device applications. *J Mater Chem C* 7:15007–15013. <https://doi.org/10.1039/c9tc04965g>
- Zhang L et al (2019c) Dual-emitting film with cellulose nanocrystal-assisted carbon dots grafted SrAl₂O₄:Eu⁽²⁺⁾, Dy⁽³⁺⁾ phosphors for temperature sensing. *Carbohydr Polym* 206:767–777. <https://doi.org/10.1016/j.carbpol.2018.11.031>
- Zhang Z, Liu G, Li X, Zhang S, Lu X, Wang Y (2020) Design and synthesis of fluorescent nanocelluloses for sensing and bioimaging applications. *ChemPlusChem* 85:487–502. <https://doi.org/10.1002/cplu.201900746>
- Zhou T, Yang Y, Zhou K, Jin M, Han M, Li W, Yin C (2019a) Efficiently mitochondrial targeting fluorescent imaging of

- H₂S invivo based on a conjugate-lengthened cyanine NIR fluorescent probe. *Sens Actuators B* 301:127116. <https://doi.org/10.1016/j.snb.2019.127116>
- Zhu L, Zhou X, Liu Y, Fu Q (2019b) Highly sensitive, ultra-stretchable strain sensors prepared by pumping hybrid fillers of carbon nanotubes/cellulose nanocrystal into electrospun polyurethane membranes. *ACS Appl Mater Interfaces* 11:12968–12977. <https://doi.org/10.1021/acsami.9b00136>
- Zhu P, Liu Y, Fang Z, Kuang Y, Zhang Y, Peng C, Chen G (2019c) Flexible and highly sensitive humidity sensor based on cellulose nanofibers and carbon nanotube composite film. *Langmuir* 35:4834–4842. <https://doi.org/10.1021/acs.langmuir.8b04259>
- Zor E, Bekar N (2017) Lab-in-a-syringe using gold nanoparticles for rapid colorimetric chiral discrimination of enantiomers. *Biosens Bioelectron* 91:211–216. <https://doi.org/10.1016/j.bios.2016.12.031>

Publisher's Note Springer Nature remains neutral with regard to jurisdictional claims in published maps and institutional affiliations.